PERGAMON

International Journal of Solids and Structures 37 (2000) 6239–6276

INTERNATIONAL JOURNAL OF SOLIDS and STRUCTURES

www.elsevier.com/locate/ijsolstr

An asymptotic analysis of delamination buckling and growth in layered plates

Domenico Bruno*, Fabrizio Greco

Department of Structural Engineering, University of Calabria, Cosenza, Italy

Received 4 December 1998; in revised form 18 May 1999

Abstract

Delamination buckling and growth in compressively loaded elastic-layered plates is analyzed. The delamination growth process is assumed to start from an initial interlaminar adhesion defect and propagate as induced by buckling. The relevant governing equations for buckling and initial postbuckling are developed by employing asymptotic analysis results. The energy release rate concept is then applied to analyze delamination growth. Two techniques are analyzed, namely the global energy approach and the local *J*-integral approach. For the two cases, the effects of the asymptotic approach accuracy on the postbuckling and delamination growth are investigated. A general model of the plate is proposed, in which a global instability of the whole plate can occur together with a local instability of the layers. In addition, simplified models are examined which may be useful in many engineering applications, although based on hypotheses about the plate geometry. Finally, the numerical results show the effectiveness of the developed models. Comparisons between the general model and the thin film approximation show the convergence of the former to the latter.

Keywords: Plates; Delamination; Buckling

1. Introduction

Composite structures exhibit notable mechanical characteristics, such as high strength-to-weight and stiffness-to-weight ratios; as a result, they are widely used in many fields of structural engineering. On the other hand, the global behaviour of such structures can be adversely affected by the presence of structural defects, such as delaminations which can arise from manufacturing processes, for instance, shocks in assembling procedures. These can drastically reduce the stiffness characteristics and the maximum load carrying capacity of the structure.

Delamination buckling and growth in composites was analyzed by Chai et al. (1981), Bottega and Maewal (1983), Yin (1985), Evans and Hutchinson (1984), Yin et al. (1986), Bruno (1988), Bruno and

* Corresponding author. Tel.: +390-984-494027; fax: +390-984-494045.
E-mail address: d.bruno@unical.it (D. Bruno).

0020-7683/00/$ - see front matter
PII: S0020-7683(99)00281-4

Grimaldi (1990), Larsson (1991), Kardomateas (1993), Sheinman and Kardomateas (1997) and Sheinman et al. (1998). In these works different approaches were used, leading in some cases to different results. Experimental results on delamination buckling were given by Kardomateas (1990) and Comiez et al. (1995).

The aim of the present paper is to investigate the delamination and growth phenomena in layered plates, as related to the analysis of the maximum load carrying capacity and structural reliability of these structures. The delamination buckling of layered plates is analyzed by modeling the delamination growth, both by the path independent integral technique, leading to a delamination condition of local type involving stresses at the crack tip, and by an approach of a global type, in which the energy release rate is evaluated as the first variation of the total potential energy with respect to the advancing delaminated area. The focus of the present analysis is, in fact, the investigation of the effects of various approximations on results obtained employing the two approaches. In particular, it will be shown that the global approach is more suitable to obtain a sufficiently accurate approximation of the delamination growth behaviour as it requires a low order asymptotic analysis.

As far as buckling and postbuckling modeling is concerned, an asymptotic analysis is performed (Britvec, 1973; Thompson and Hunt, 1973). Developments are addressed to the narrow-plate and to the axisymmetric circular-plate structural schemes which can capture the main features of the delamination process phenomenon. Even if the analysis is carried out for homogeneous and isotropic elastic layered plates the results can be, in principle, extended to the general case of anisotropic layers with different mechanical characteristics.

A general model of the plate is analyzed, without restrictive assumptions on the plate geometry. For this model, global buckling of the plate can occur accompanied by a local instability of delaminated layers. Some simplified models based on restrictive hypotheses on geometry and deformation of the plate (thick column, thin film, and symmetric split models) are also analyzed by the same approach, leading to results which may be of interest in view of practical engineering applications. Moreover, the effectiveness of the general model and the coherence of the basic asymptotic expansion equations are validated showing convergence of the general model to the thin film approximation. The influence on the solution of the asymptotic expansion terms is investigated and the effects on energy release rate evaluation are evidenced.

It is possible to conclude from our results that the global approach in which the energy release rate is evaluated as a function of the total potential energy of the system is the most appropriate, because this can capture the main nonlinearities of the behaviour. In fact, if the energy approach is used, lower order terms need to be considered in the asymptotic expansion of load and displacement to achieve a reasonable asymptotic approximation of the energy release rate. In contrast, in instances where the energy release rate concept is applied involving stresses at the crack tip, the same accuracy can be obtained only if higher order stress terms are considered in the asymptotic expansion, particularly if there is notable stiff postbuckling behaviour of the structure. A relevant conclusion of this paper is that an appropriate accuracy in the postbuckling modeling is required to study delamination buckling and growth; otherwise, in many cases imprecise results may be found, possibly implying an overestimation of the stiffness and of the strength of the structure. For instance, neglecting of higher-order terms in the asymptotic approximation of stresses may lead to a stiffness and strength overestimation, especially in the limit cases of thin film and symmetric split models.

2. The initial postbuckling and delamination growth models

A typical delamination buckling behaviour of a delaminated plate is shown in Fig. 1, where a two-

layer narrow plate scheme with an initial bonding defect of size ℓ_0 and subjected to an axial compression N, is considered. The load-displacement equilibrium path is plotted in terms of the axial compression N as a function of the axial relative end displacement Δ.

For this scheme, several instability phenomena can arise depending on the plate geometry. Short and thick initial defects (i.e. small values of the length-to-thickness ratio of the delaminated layer) scarcely influence the buckling load of the plate and the rule is an overall instability in which the postbuckling behaviour is characterized by a drastic reduction of stiffness.

On the contrary, long and thin initial defects drastically reduce the buckling load of the plate. In this case, in fact, the upper layer undergoes a state of local buckling and the delamination area may subsequently spread. For different sizes of initial defects, a narrow transition zone may exist in which a global instability of the whole plate is accompanied with a local instability of layers.

In the general case of arbitrary initial defect and when N reaches the critical value N_c, the plate undergoes buckling with every plate element deflected in the same direction, but shortly after buckling, a

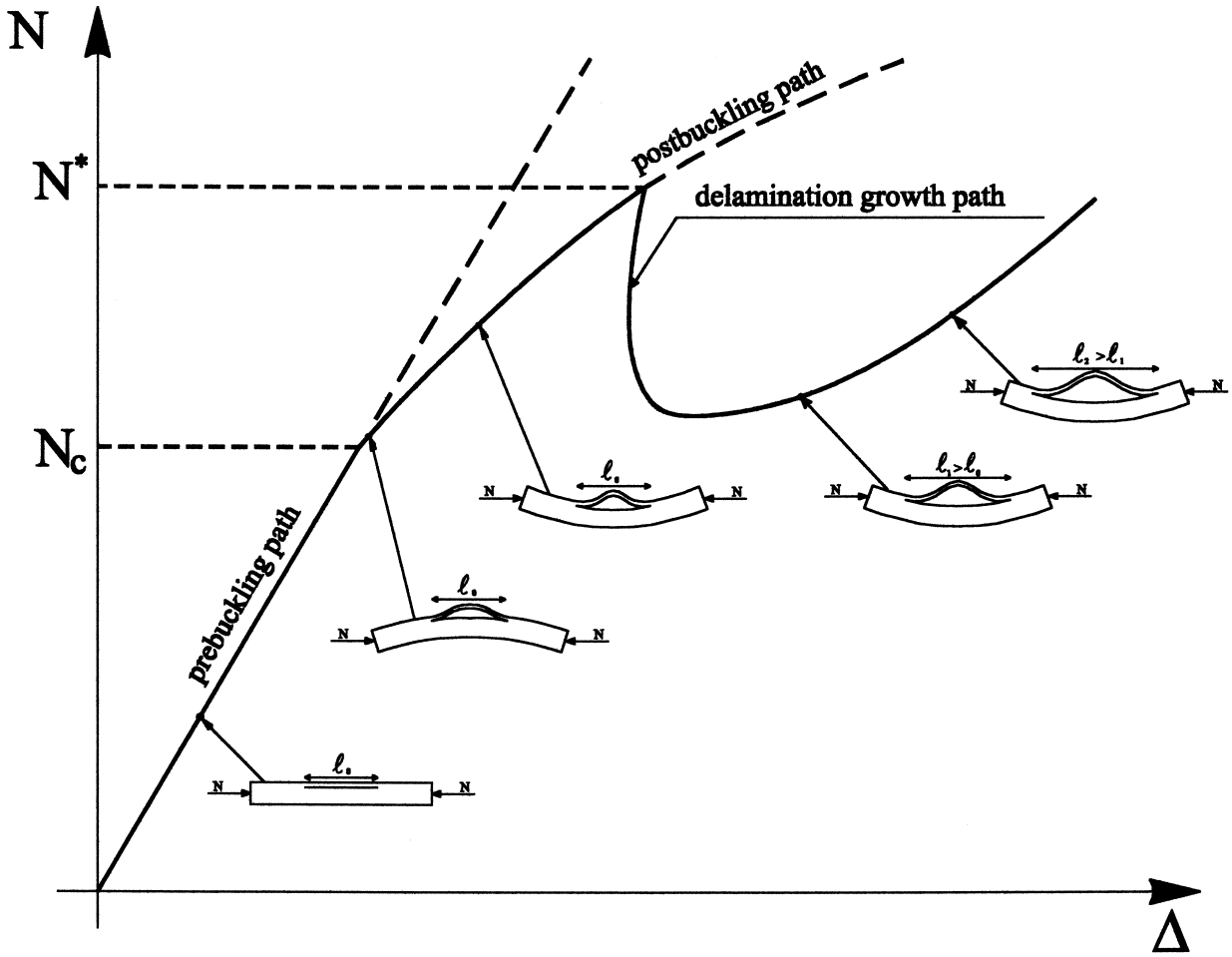

Fig. 1. Delamination scheme of a plate.

snap-through may occur and the delamination becomes fully open. Eventually, the external load N can increase until a limit value N^* is reached, at which the delamination process starts.

The delamination growth path sketched in Fig. 1 is of a general type and its characteristics depend on various geometrical and mechanical parameters (see Chai et al., 1981). On the other hand, the actual behaviour is more complex due to a number of causes, such as geometrical imperfections, damage of the material, etc. For instance, in the experimental work of Kardomateas (1990) a transition from unstable to stable behaviour was not found for the delamination growth path.

In this work, the delamination buckling and growth behaviour of an elastic plate containing an initial defect is analyzed by using a general asymptotic approach in which the initial postbuckling results, in the form presented by Budiansky (1974), are combined with those of elastic brittle fracture mechanics. We therefore propose a generalization of the approach of Bruno and Grimaldi (1990), where the analysis was restricted to the simple symmetric split scheme. In particular, as far as the initial postbuckling analysis is concerned, the perturbation approach proposed by Budiansky is employed by assuming the following asymptotic expansion of the generalized displacements u and of the load multipier λ

$$u = u_0(\lambda) + u_1\varepsilon + u_2\varepsilon^2 + u_3\varepsilon^3 + u_4\varepsilon^4 + \cdots \tag{1}$$

$$\lambda = \lambda_c + \lambda_1\varepsilon + \lambda_2\varepsilon^2 + \lambda_3\varepsilon^3 + \lambda_4\varepsilon^4 + \cdots, \tag{2}$$

where ε is a perturbation parameter, $u_0(\lambda)$ the prebuckling fundamental displacement solution, λ_c the buckling load, u_1 the buckling mode, $\lambda_1, \lambda_2, \ldots$ and $u_2, u_3, \ldots$ are postbuckling load coefficients and displacement increments.

As far as the delamination condition is concerned, the Griffith criterion is employed to model the delamination growth process. In this context, if we consider a two-layer plate with an initial bonding defect occupying an area A_0 with outer boundary C_0 (Fig. 2), the monotonic growth of delamination from the initial outer boundary C_0 to the actual C with an infinitesimal increment ΔA of delaminated area, is governed by the following equation

$$\lim_{\Delta A \to 0} \frac{[\Phi + B]_{C_0}^{C}}{\Delta A} = 0 \tag{3}$$

where $\Phi = W - L$ is the total potential energy of the system, W is the strain energy, and L the work performed by the applied loads, while B is the energy spent in increasing the delaminated area.

If the adhesion between the layers is modelled by a surface adhesion energy parameter Γ, Eq. (3) becomes $G = \Gamma$, where

$$G = -\lim_{\Delta A \to 0} \frac{[\Phi]_{C_0}^{C}}{\Delta A}, \tag{4}$$

is the energy release rate.

In the case of delamination buckling, the increment $\Delta\Phi$ of the total potential energy from the prebuckling configuration is only involved in Eq. (3). It is assumed that this energy increment $\Delta\Phi(u, \lambda)$ has a Taylor expansion from the prebuckling configuration. In addition, it is assumed that $\Delta\Phi(u, \lambda)$ is a linear function of the load parameter λ

$$\Delta\Phi(u, \lambda) = \Delta\Phi(u, \lambda_c) + (\lambda - \lambda_c)\Delta\dot{\Phi}(u, \lambda_c),$$

where $\Delta\dot{\Phi}(u, \lambda_c) = [\mathrm{d}\Delta\Phi(u, \lambda)/\mathrm{d}\lambda]_{\lambda=\lambda_c}$. Moreover, $\Delta\Phi$ can be cast in the following form

$$\Delta\Phi = \frac{1}{2}\left[\Delta\Phi_c^{\mathrm{II}} + \Delta\lambda\Delta\dot{\Phi}_c^{\mathrm{II}}\right]\Delta u^2 + \frac{1}{6}\left[\Delta\Phi_c^{\mathrm{III}} + \Delta\lambda\Delta\dot{\Phi}_c^{\mathrm{III}}\right]\Delta u^3 + \frac{1}{24}\left[\Delta\Phi_c^{\mathrm{IV}} + \Delta\lambda\Delta\dot{\Phi}_c^{\mathrm{IV}}\right]\Delta u^4 + \cdots \tag{5}$$

where $\Delta u = u - u_0 = u_1\varepsilon + u_2\varepsilon^2 + u_3\varepsilon^3 + \cdots$ is the displacement increment, and $\Delta\lambda = \lambda - \lambda_c$ is the load increment from the critical state. Moreover, the prime denotes the derivative of the increment of the total potential energy $\Delta\Phi$, evaluated at the critical configuration, i.e. at $\lambda = \lambda_c$, with respect to the displacement variable u, with the meaning $\Delta\Phi^N = \Delta\Phi^N[u_0(\lambda_c), \lambda_c]$.

If a symmetric postbuckling occurs, as in the case of most of our example problems, using the asymptotic expansions Eqs. (1) and (2), the energy $\Delta\Phi$ can be written in an appropriate asymptotic form

$$\Delta\Phi = \left(\Delta\dot{\Phi}_c^{\mathrm{II}}\frac{u_1^2}{2}\lambda_2 + \Delta\Phi_c^{\mathrm{IV}}\frac{u_1^4}{24}\right)\varepsilon^4 + \left(\Delta\Phi_c^{\mathrm{VI}}\frac{u_1^6}{720} + \Delta\dot{\Phi}_c^{\mathrm{IV}}\frac{u_1^4}{24}\lambda_2 + \Delta\Phi_c^{\mathrm{IV}}\frac{u_1^3u_3}{6} + \Delta\dot{\Phi}_c^{\mathrm{II}}\frac{u_1^2}{2}\lambda_4 + \Delta\dot{\Phi}_c^{\mathrm{II}}u_1u_3\lambda_2 + \Delta\Phi_c^{\mathrm{II}}\frac{u_3^2}{2}\right)\varepsilon^6 + \mathrm{O}(\varepsilon^8). \tag{6}$$

The delamination condition can be applied directly in the original form (3) in which the total potential energy of the system is taken into consideration and global quantities are involved. In addition, an alternative approach can be used in which generalized in-layer stresses at the delamination tip are employed as a result of the application of path-independent integrals. For plane strain or generalized plane stress problems, such as the narrow plate scheme, the energy release rate can be calculated with the aid of the J-integral (Rice, 1968)

$$G = J = \int_C \left(W\mathrm{d}x_2 - T_i\frac{\partial u_1}{\partial x_1}\mathrm{d}s\right), \tag{7}$$

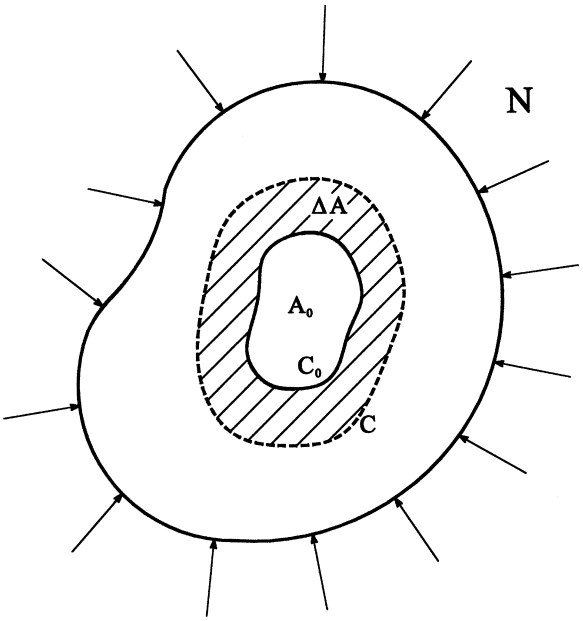

Fig. 2. Delaminated plate: plane view.

where C is a curve surrounding the crack tip, T_i is the traction acting on the outerside C, W is the strain energy density and (x_1, x_2) is an orthogonal reference system with x_1-axis coincident with the crack direction. To avoid the effects of singularities in stress distribution, curve C is chosen at a suitable distance from the crack tip.

For axisymmetric problems, analogous results have been obtained by Budiansky and Rice (1973), by expressing the energy release rate as a function of the M-integral, in the following form

$$G = \frac{M}{2\pi R_c^2}, \qquad M = 2\pi \int_A \left[W x_i n_i - T_i u_{i,j} x_j - T_i \frac{u_i}{2} \right] r \, \mathrm{d}s, \quad i,j = r,z, \tag{8}$$

where A is a torus-like surface ringing the edge of the axisymmetric delamination, r and z are cylindrical coordinates with the z-axis being the axis of revolution and the r-axis being located in the crack plane.

3. Narrow plate model

In this section a one-dimensional model is analyzed, considering a two-layer plate of length L and width B. At the interface between the two layers, a through-width delamination of length ℓ_0 is present, and the plate is loaded in compression by an axial force N, as shown in Fig. 3. The unbounded part of the plate of thickness T and length $b = (L - \ell)/2$ is referred to as the base layer, the layers above and below the delamination zone (referred to as the delaminated and substrate layer), have thickness t and H, respectively. Several schemes are developed and analyzed by incorporating in the analysis some inherent approximations leading to simple formulas. These are (i) the thin film model ($t/T \to 0$), (ii) the thick column model ($t/T \ll 1$), and (iii) the symmetric split model ($t/T = 0.5$).

In addition, a general model, free of restrictive assumptions for the plate geometry, is also developed and the convergence of this model to the limit case of thin film model is shown. For simplicity, the layers are assumed to be homogeneous, isotropic and linearly elastic.

The initial postbuckling and delamination growth behaviour of the narrow plate is analyzed through a perturbation procedure by combining results of the elastica theory (Britvec, 1973) and of brittle elastic fracture mechanics.

Load and deformation quantities of an elastic beam member depend essentially on three independent variables: a distortion parameter and two amplitudes (Britvec, 1973). Exact dependence is given by means of elliptic functions, while if an approximate asymptotic expansion is used, this dependence is established in terms of trigonometric functions.

In order to show the influence of the postbuckling modeling accuracy on the prediction of the delamination process, investigations are performed on the effects of energy and stress terms of the asymptotic expansion governing delamination growth. In addition, some comparisons with exact solutions are also given (when these are available).

For our one-dimensional problem, the delamination condition (3) can be written in the following form

$$G = -\frac{\partial \Delta \Phi}{B \partial \ell} = \Gamma \tag{9}$$

where Γ is the surface adhesion energy between layers, $\Delta\Phi$ the increment of the total potential energy as shown (Fig. 4), N the applied compression and u_L is the corresponding axial shortening.

The energy $\Delta\Phi$ can be evaluated with the aid of Eq. (5) or directly by integrating the area depicted in Fig. 4.

As discussed in the previous section, the energy release rate G can also be calculated with the aid of

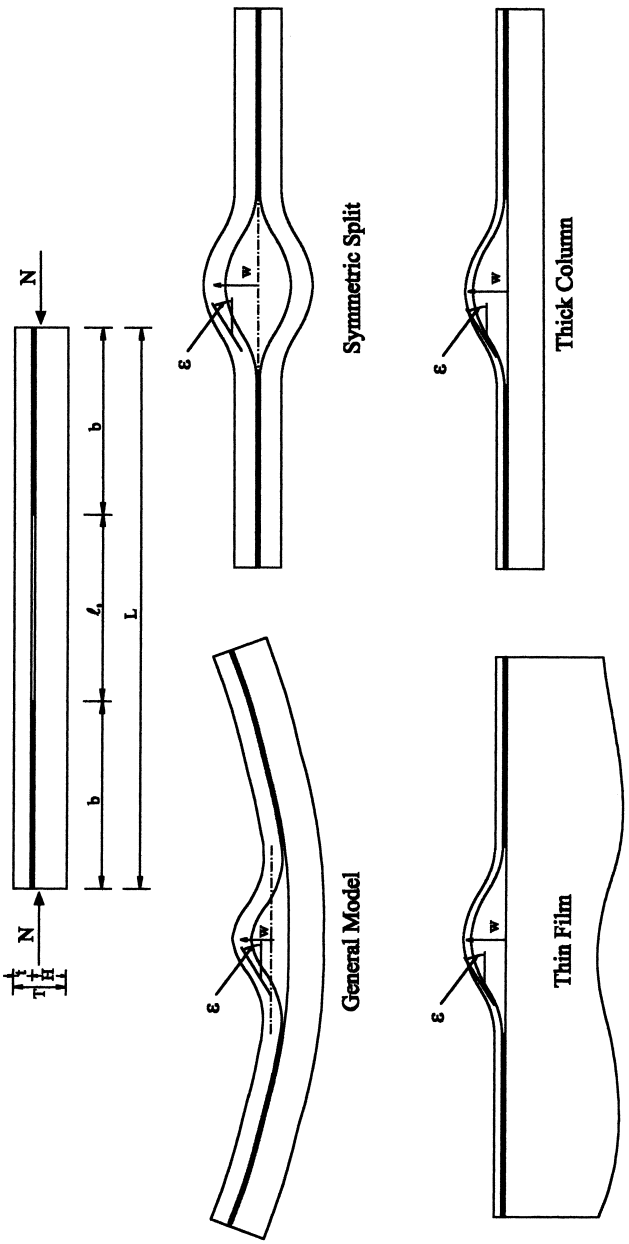

Fig. 3. Geometry and delamination-buckling schemes of the narrow plate model.

the J-integral concept. For a one-dimensional beam model, Yin and Wang (1984) obtained an algebraic expression for the energy release rate G in terms of bending and axial stresses at the crack tip. The method is sketched in Fig. 5, where it is shown that stresses at the crack tip are partitioned into two stress subsystems (a) and (b). Note that only the latter (P^*, M^l, M^u) produces a singular stress field.

The energy release rate can be calculated by using the J-integral

$$G = \frac{1}{2B}\left[\frac{(P^*)^2}{A_u} + \frac{(P^*)^2}{A_l} + \frac{(M^{\mathrm{u}})^2}{D_u} + \frac{(M^{\mathrm{l}})^2}{D_l}\right], \tag{10}$$

where A_{u}, A_{l}, D_{u} and D_{l} are the bending and axial stiffness of the upper and lower delaminated layer, respectively.

3.1. General model

This model has also been analyzed by Chai et al. (1981), Yin et al. (1986) and Kardomateas (1993). In the first and second works the buckling and postbuckling behaviour is analyzed by modeling the plate as composed of nonlinear beam column elements and some approximations in the kinematics are introduced through trigonometric functions for transverse deflections. The energy release rate is calculated by means of numerical differentiation in Chai et al. (1981), and applying the method of J-integral (Yin et al., 1986) in a form derived by Yin and Wang (1984). In Kardomateas (1993), the analysis is carried out by a second order perturbation analysis based on the results given by Britvec (1973), relative to the elastica theory.

Here we extend the analysis performed by Kardomateas (1993), using a refined asymptotic expansion. A perturbation procedure to construct the relevant governing equations of the model is developed. In the following, the subscript i = d, s, b refers to the delaminated, substrate and base layer, respectively. The analysis is presented both for simply supported and clamped boundary conditions.

Every layer of the plate is considered as a compressive elastic member, restrained by means of concentrated forces and moments. The asymptotic expansion of the load and deformation quantities in terms of the distortion parameter of the delaminated layer, is performed and the postbuckling solution is analyzed through the compatibility and equilibrium conditions at the common section.

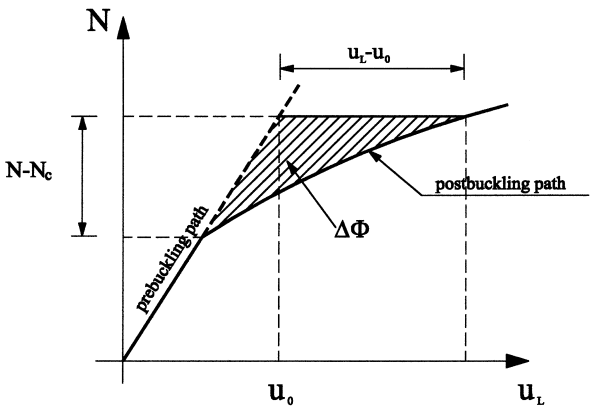

Fig. 4. Total potential energy increment.

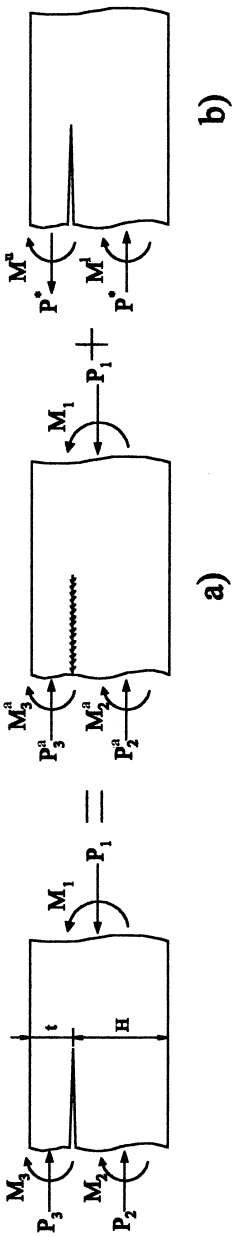

Fig. 5. Superposition scheme of stresses at the crack tip.

3.1.1. Delaminated layer

The delaminated layer is treated as a part of an elastica. The buckled configuration, due to its symmetry with respect to the midsection of the plate (Fig. 6), is defined by the end amplitude Φ_d and distortion parameter ε. For symmetric elements, in fact, the relation $\Phi_i = -\Phi_j$ holds true and the end rotation is obtained by expanding the exact expression in Taylor series about the critical state in terms of the distortion parameter ε. This represents the tangent rotation at the inflection point from the straight position, positive if clockwise

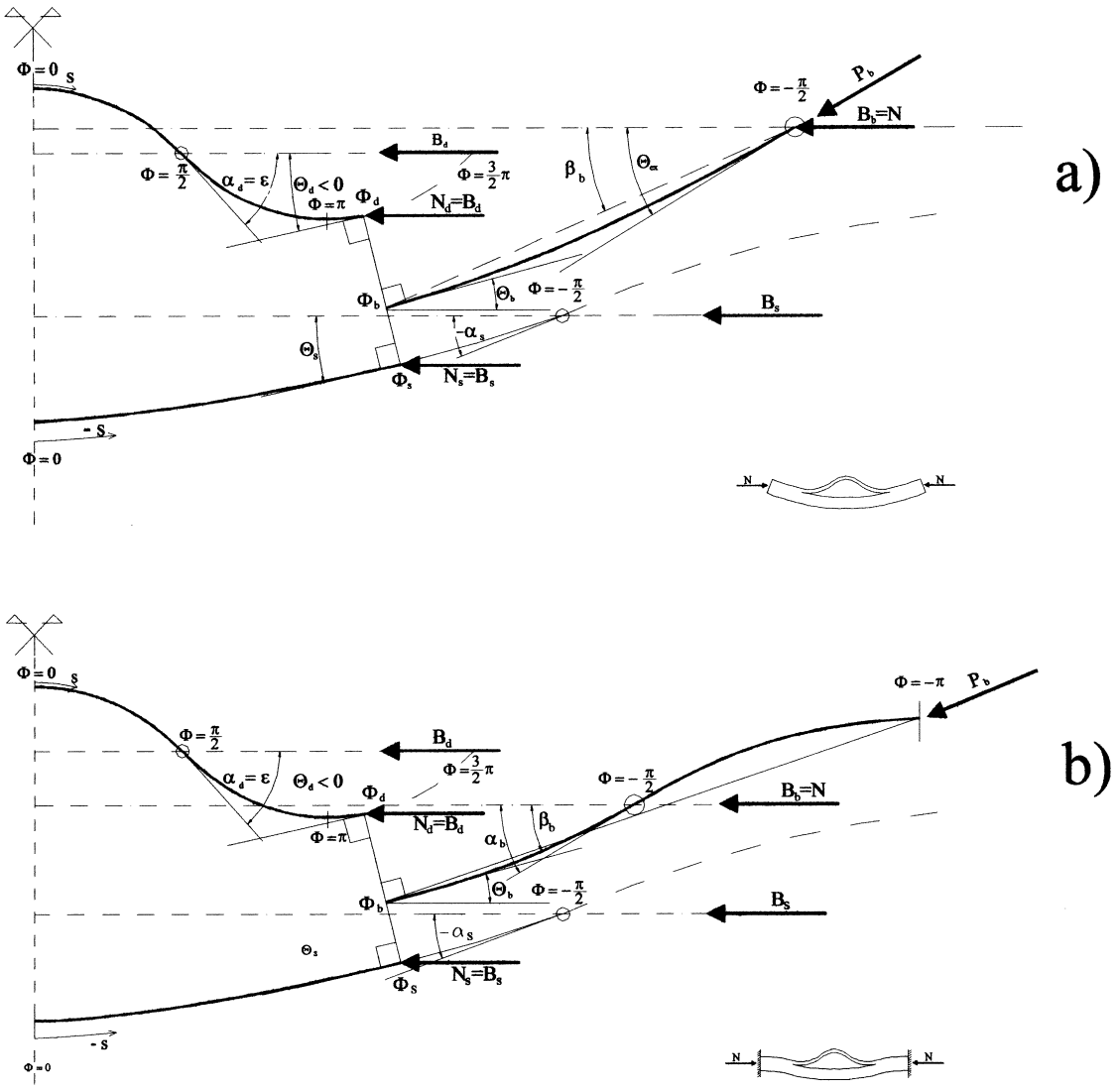

Fig. 6. Buckled configuration of the elastica curves representing the constitutive elements of the delaminated plate (symmetric part): (a) simply supported plate and (b) clamped plate.

$$\theta_d = \sin(\Phi_d)\varepsilon - \frac{1}{24}\big(\sin(\Phi_d)\cos^2(\Phi_d)\big)\varepsilon^3 + O(\varepsilon^5). \tag{11}$$

At the critical state, the end amplitude Φ_d can be expanded in the form

$$\Phi_d = \Phi_d^0 + \Phi_d^{(1)}\varepsilon + \Phi_d^{(2)}\varepsilon^2 + \Phi_d^{(3)}\varepsilon^3 + O(\varepsilon^4); \tag{12}$$

therefore, the tangent rotation becomes:

$$\theta_d = \big(\sin\Phi_d^0\big)\varepsilon + \big(\cos\Phi_d^0\big)\Phi_d^{(1)}\varepsilon^2 + \left[\cos\Phi_d^0\Phi_d^{(2)} - \sin\Phi_d^0\frac{\Phi_d^{(1)2}}{2} - \frac{1}{24}\sin\Phi_d^0\cos^2\Phi_d^0\right]\varepsilon^3 + \left[\cos\Phi_d^0\Phi_d^{(3)}\right.$$
$$\left. - \sin\Phi_d^0\Phi_d^{(1)}\Phi_d^{(2)} - \frac{1}{24}\Big(\Phi_d^{(1)}\cos^3\Phi_d^0 - 2\Phi_d^{(1)}\cos\Phi_d^0\sin^2\Phi_d^0\Big) - \frac{\Phi_d^{(1)3}\cos\Phi_d^0}{6}\right]\varepsilon^4 + O(\varepsilon^5),$$

or in compact form

$$\theta_d = \theta_d^{(1)}\varepsilon + \theta_d^{(2)}\varepsilon^2 + \theta_d^{(3)}\varepsilon^3 + \theta_d^{(4)}\varepsilon^4 + O(\varepsilon^5). \tag{13}$$

In a similar way, we proceed for the end moment M_d, the axial force N_d and the flexural contraction f_d

$$M_d = M_d^{(1)}\varepsilon + M_d^{(2)}\varepsilon^2 + M_d^{(3)}\varepsilon^3 + M_d^{(4)}\varepsilon^4 + O(\varepsilon^5), \tag{14}$$

$$N_d = N_d^0 + N_d^{(1)}\varepsilon + N_d^{(2)}\varepsilon^2 + N_d^{(3)}\varepsilon^3 + O(\varepsilon^4), \tag{15}$$

$$f_d = f_d^{(2)}\varepsilon^2 + f_d^{(3)}\varepsilon^3 + f_d^{(4)}\varepsilon^4 + O(\varepsilon^5). \tag{16}$$

3.1.2. Substrate layer

The end amplitude Φ_s and the distortion parameter α_s are now expanded with respect to the distortion parameter of the delaminated layer ε

$$\Phi_s = \Phi_s^0 + \Phi_s^{(1)}\varepsilon + \Phi_s^{(2)}\varepsilon^2 + \Phi_s^{(3)}\varepsilon^3 + O(\varepsilon^4), \tag{17}$$

$$\alpha_s = \alpha_s^{(1)}\varepsilon + \alpha_s^{(2)}\varepsilon^2 + \alpha_s^{(3)}\varepsilon^3 + \alpha_s^{(4)}\varepsilon^4 + O(\varepsilon^5). \tag{18}$$

The end rotation θ_s, the end moment M_s, the axial force N_s and the flexural f_s can be found once more by expanding the relevant expressions (Britvec, 1973)

$$\theta_s = \theta_s^{(1)}\varepsilon + \theta_s^{(2)}\varepsilon^2 + \theta_s^{(3)}\varepsilon^3 + \theta_s^{(4)}\varepsilon^4 + O(\varepsilon^5) \tag{19}$$

$$M_s = M_s^{(1)}\varepsilon + M_s^{(2)}\varepsilon^2 + M_s^{(3)}\varepsilon^3 + M_s^{(4)}\varepsilon^4 + O(\varepsilon^5), \tag{20}$$

$$N_s = N_s^0 + N_s^{(1)}\varepsilon + N_s^{(2)}\varepsilon^2 + N_s^{(3)}\varepsilon^3 + O(\varepsilon^4), \tag{21}$$

$$f_s = f_s^{(2)}\varepsilon^2 + f_s^{(3)}\varepsilon^3 + f_s^{(4)}\varepsilon^4 + O(\varepsilon^5). \tag{22}$$

3.1.3. Base layer

The load and deformation quantities for the base layer are influenced by the external boundary conditions, thus the amplitude at the simply supported end is $-\pi/2$ while at the clamped end is $-\pi$. The amplitude at the common section and the distortion parameter of the base layer are

$$\Phi_b = \Phi_b^0 + \Phi_b^{(1)}\varepsilon + \Phi_b^{(2)}\varepsilon^2 + \Phi_b^{(3)}\varepsilon^3 + O(\varepsilon^4), \tag{23}$$

$$\alpha_b = \alpha_b^{(1)}\varepsilon + \alpha_b^{(2)}\varepsilon^2 + \alpha_b^{(3)}\varepsilon^3 + \alpha_b^{(4)}\varepsilon^4 + O(\varepsilon^5). \tag{24}$$

The asymptotic expressions for load and deformation quantities are

$$\theta_b = \theta_b^{(1)}\varepsilon + \theta_b^{(2)}\varepsilon^2 + \theta_b^{(3)}\varepsilon^3 + \theta_b^{(4)}\varepsilon^4 + O(\varepsilon^5), \tag{25}$$

$$M_b = M_b^{(1)}\varepsilon + M_b^{(2)}\varepsilon^2 + M_b^{(3)}\varepsilon^3 + M_b^{(4)}\varepsilon^4 + O(\varepsilon^5), \tag{26}$$

$$N = N^0 + N^{(1)}\varepsilon + N^{(2)}\varepsilon^2 + N^{(3)}\varepsilon^3 + O(\varepsilon^4), \tag{27}$$

$$f_b = f_b^{(2)}\varepsilon^2 + f_b^{(3)}\varepsilon^3 + f_b^{(4)}\varepsilon^4 + O(\varepsilon^5). \tag{28}$$

The nonlinear postbuckling path is defined by equilibrium and compatibility requirements at the common section.

3.1.4. Equilibrium equations

The force and moment equilibrium are

$$N_d + N_s - N = 0, \tag{29}$$

$$M_d + M_s + M_b - N_d\frac{H}{2}\cos\theta + N_s\frac{t}{2}\cos\theta = 0; \tag{30}$$

where: $\cos\theta = 1 - \theta^{(1)2}\frac{\varepsilon^2}{2} - \theta^{(1)}\theta^{(2)}\varepsilon^3$.

3.1.5. Compatibility equations

The continuity condition for the rotation at the common section requires

$$\theta_d = \theta_s = \theta_b. \tag{31}$$

Moreover, axial shortening, due to both axial and flexural deformations, for the delaminated and substrate layer must be compatible

$$\left[f_d + \frac{N_d\ell(1-\upsilon^2)}{EBt}\right] - \left[f_s + \frac{N_s\ell(1-\upsilon^2)}{EBH}\right] + \sin\theta\cdot(H+t) = 0; \tag{32}$$

where:

$$\sin\theta = \sin\Phi_d^0\varepsilon + \Phi_d^{(1)}\cos\Phi_d^0\varepsilon^2 + \left(\Phi_d^{(2)}\cos\Phi_d^0 - \frac{\Phi_d^{(1)2}\sin\Phi_d^0}{2} - \frac{\cos^2\Phi_d^0\sin\Phi_d^0}{24} - \frac{\sin^3\Phi_d^0}{6}\right)\varepsilon^3 + \cdots.$$

The first order equilibrium and compatibility conditions define the critical state. The second, third and fourth order equations provide the corresponding first, second and third order forces.

3.1.6. Displacement parameters

The expression for the applied compressive displacement is

$$u = \left[f_{\mathrm{d}} + \frac{N_{\mathrm{d}}\ell(1-\nu^2)}{EBt}\right] + \left[2f_{\mathrm{b}} + \frac{2Nb(1-\nu^2)}{EBT}\right] + \sin\theta T = \frac{N^0 L(1-\nu^2)}{EBT} + \Big(\frac{2N^{(1)}b(1-\nu^2)}{EBT} + \frac{N_{\mathrm{d}}^{(1)}\ell(1-\nu^2)}{EBt} + H\theta^{(1)}\Big)\varepsilon + \left\{f_{\mathrm{d}}^{(2)} + \frac{N_{\mathrm{d}}^{(2)}\ell(1-\nu^2)}{EBt} + 2f_{\mathrm{b}}^{(2)} + \frac{2N^{(2)}b(1-\nu^2)}{EBT} + H\theta^{(2)}\right\}\varepsilon^2 + \cdots. \tag{33}$$

The midpoint deflection of the delaminated layer is given by

$$w_{\mathrm{dm}} = w_{\mathrm{dm}}^{(1)}\varepsilon + w_{\mathrm{dm}}^{(2)}\varepsilon^2; \tag{34}$$

where

$$w_{\mathrm{dm}}^{(1)} = \frac{\ell}{2\Phi_{\mathrm{d}}^0}\big(1-\cos\Phi_{\mathrm{d}}^0\big), \qquad w_{\mathrm{dm}}^{(2)} = \frac{\ell}{2\Phi_{\mathrm{d}}^0}\left(\frac{\cos\Phi_{\mathrm{d}}^0 - 1}{\Phi_{\mathrm{d}}^0} + \sin\Phi_{\mathrm{d}}^0\right)\Phi_{\mathrm{d}}^{(1)}; \tag{35}$$

and that of the substrate layer

$$w_{\mathrm{sm}} = w_{\mathrm{sm}}^{(1)}\varepsilon + w_{\mathrm{sm}}^{(2)}\varepsilon^2, \tag{36}$$

$$w_{\mathrm{sm}}^{(1)} = \frac{\ell}{2\Phi_{\mathrm{s}}^0}\big(1-\cos\Phi_{\mathrm{s}}^0\big)\alpha_{\mathrm{s}}^{(1)}, \tag{37}$$

$$w_{\mathrm{sm}}^{(2)} = \frac{\ell}{2\Phi_{\mathrm{s}}^0}\left(\frac{\cos\Phi_{\mathrm{s}}^0 - 1}{\Phi_{\mathrm{s}}^0} + \sin\Phi_{\mathrm{s}}^0\right)\Phi_{\mathrm{s}}^{(1)}\alpha_{\mathrm{s}}^{(1)} + \frac{\ell}{2\Phi_{\mathrm{s}}^0}\big(1-\cos\Phi_{\mathrm{s}}^0\big)\alpha_{\mathrm{s}}^{(2)}. \tag{38}$$

The representation of the assembled elastica curves for both the simply supported (case a) and the clamped boundary (case b) restraint conditions are shown in Fig. 6.

From the analysis developed in the previous section, it follows that the buckling mode is defined by a critical end-amplitude $\pi/2 < \Phi_{\mathrm{d}}^0 < \pi$ for the delaminated layer, which therefore shows a symmetric inflection point, while for the substrate layer we have $-\pi/2 < \Phi_{\mathrm{s}}^0 < 0$, with no inflection point and for the base layer $-\pi/2 < \Phi_{\mathrm{b}}^0 < 0$ and $-\pi < \Phi_{\mathrm{b}}^0 < 0$ referred to as the simply supported and clamped conditions, respectively.

From our results the following considerations emerge. The buckling and postbuckling behaviour largely depends on the relative thickness and length of the delaminated layer, defined by the ratios $\bar{t} = t/T$ and $\bar{\ell} = \ell/L$. Introducing the dimensionless parameter of the relative slenderness of the delaminated layer with respect to the perfect plate, as

$$s = \frac{\ell T}{tL}, \tag{39}$$

we can distinguish between two very different behaviours in the two cases of short and long

delaminations. These can be approximately defined by $s < 2$ and $s > 2$ for the simply supported condition, or $s < 1$ and $s > 1$ for the clamped condition (see also Yin et al., 1986).

For short delaminations the buckling load changes slightly from that of the whole perfect plate. In fact, the loss in stiffness is small and, assuming $t/T < 0.5$, the initial amplitude of the delaminated layer is greater than that of the substrate, with an upward deflection of the plate. In the postbuckling range, the compressive load in the delaminated layer decreases while increases in the substrate, until the delamination becomes completely closed with a consequent contact between layers. This contact condition is expressed in terms of midpoint displacements by

$$w_{\mathrm{d}} + \frac{T}{2}\cos\theta_{\mathrm{d}} = w_{\mathrm{s}} + \frac{T}{2}, \tag{40}$$

or, in an asymptotic form

$$w_{\mathrm{d}}^{(1)}\varepsilon + w_{\mathrm{d}}^{(2)}\varepsilon^2 - \left(w_{\mathrm{s}}^{(1)}\varepsilon + w_{\mathrm{s}}^{(1)}\varepsilon^2 + \frac{T}{4}\theta^{(1)2}\varepsilon^2\right) = 0. \tag{41}$$

This phase can occur in the postbuckling range of the plate, which is unstable when the axial load goes beyond a maximum value (Figs. 7 and 8). In fact, the load reaches its maximum value near the critical point and then decreases as a consequence of the large negative value of the second order term $N^{(2)}$ of the load asymptotic expansion. The typical load-displacement curves are shown in Figs. 7(a) and (b) and 8(a) and (b).

For long delaminations, the critical load of the plate is drastically reduced due to the slenderness of the delaminated layer. In this case the plate buckles with a deformation mode similar to that found for short delaminations (Fig. 9(a) and (b)1). But, with a small increase in the load, the deformation shape may jump to a new configuration (Fig. 9(a)–(b)2), at which the delamination zone is fully open and may grow.

It is evident that long delaminations determine a drastic reduction of the buckling load, but the stiffness of the plate shows only a slight decrement and the maximum load-carrying capacity is not reached.

Moreover, as we can see from Figs. 7 and 8, short delaminations cause a global buckling with a value

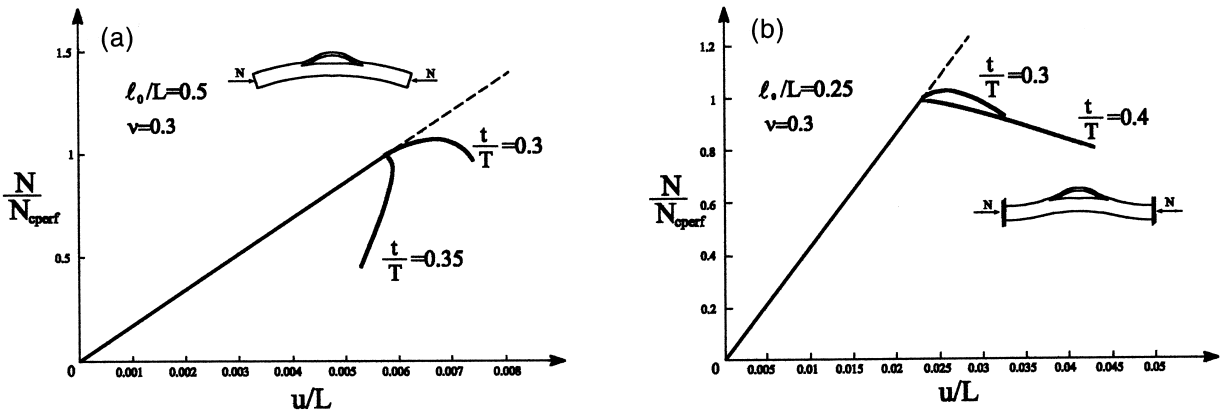

Fig. 7. Load-displacement curves for short delaminations (N: applied load; N_{cperf}: critical load of the perfect plate; u: axial shortening). (a) Simply supported plate: $s = 1.43, 1.67$, (b) clamped plate: $s = 0.833, 0.625$.

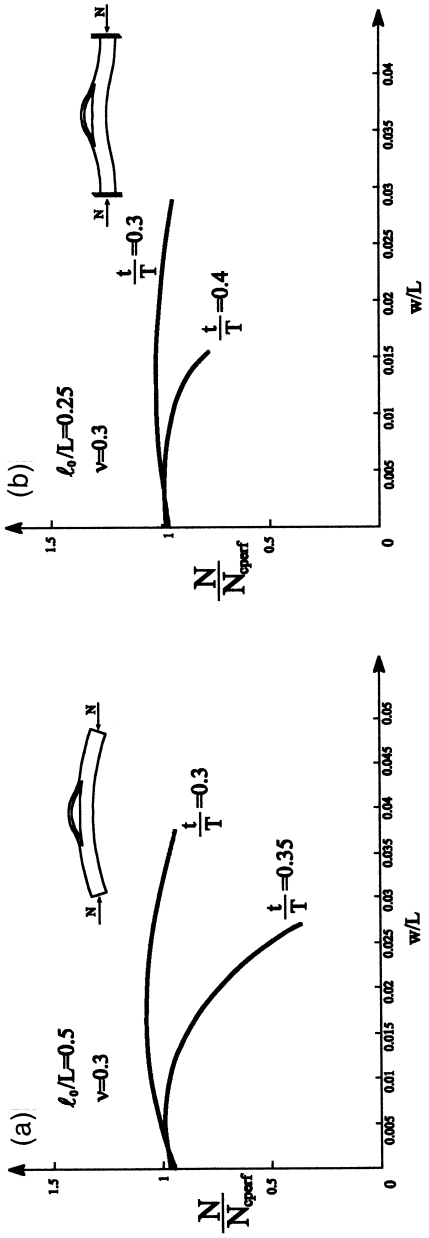

Fig. 8. Load-displacement curves for short delaminations. (N: applied load; N_{cperf}: critical load of the perfect plate; w: transverse deflection of the upper layer). (a) Simply supported plate: $s = 1.43, 1.67$, (b) clamped plate: $s = 0.833, 0.625$.

of critical load scarcely influenced by the presence of the interlaminar defect, while buckling is local and the boundary conditions scarcely affect the critical load for long delaminations.

The influence of the geometrical parameters on the buckling load is shown in Fig. 10. It can be observed that the transition value between short and long delaminations occurs approximatively at $s = 2$ or $s = 1$ for simply supported and clamped boundary conditions, respectively.

Denoting by $\bar{\ell}^* = \ell^*/L$, the normalized inflection length of the undamaged plate, the transition condition can be expressed in the form

$$s = 2 \cdot \bar{\ell}^* \tag{42}$$

for both simply supported and clamped conditions.

Similar conclusions have been obtained by Yin (1985) and Larsson (1991) by using different approaches. Moreover, some experimental results on the postbuckling behaviour of delaminated plates are given by Kardomateas (1990). These results can refer to long delaminations ($s > 1$ clamped plate) and consequently they agree with our predictions.

3.1.7. The energy release rate

The energy release rate is here calculated both through the increment of the total potential energy and by the *J*-integral. However, it must be observed that for the general model the relevant buckling governing equations does not admit a closed-form solution. Therefore, it is not possible to give an algebraic development for $\Delta\Phi$ Hence, it is calculated by means of standard numerical differentiation, while *J*-integral is applied by utilizing both second and third order postbuckling results. Let us consider the second order approximation in terms of the perturbation parameter ε of the parametric load–displacement relation

$$N = N^0 + N^{(1)}\varepsilon + N^{(2)}\varepsilon^2 + \cdots, \tag{43}$$

$$u = u^0 + u^{(1)}\varepsilon + u^{(2)}\varepsilon^2 + \cdots. \tag{44}$$

When ε is expressed as a function of u by solving the second order equation (44) and taking the positive root,

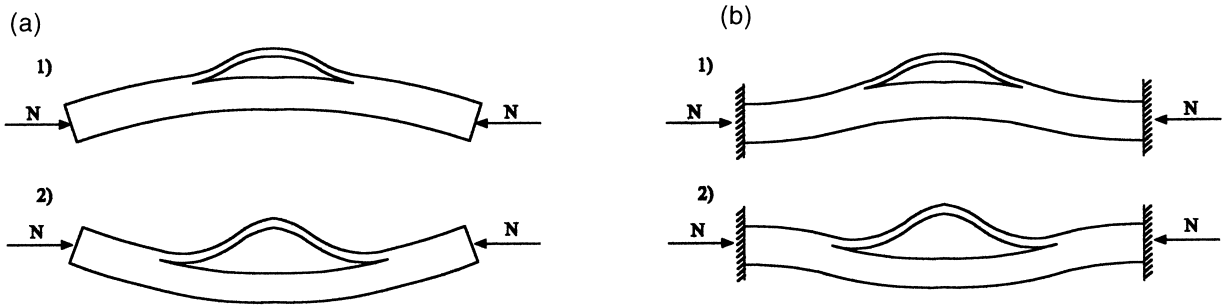

Fig. 9. (a) Deformation modes in the postbuckling range (supported end restraints). (b) Deformation modes in the postbuckling range (clamped end restraints).

$$\varepsilon = \frac{-u^{(1)} + \sqrt{u^{(1)2} + 4u^{(2)}(u - u^0)}}{2u^{(2)}} \tag{45}$$

we obtain the explicit second order approximation of the load–displacement relation.

The total potential energy increment is

$$\Delta\Phi = -\int_{N^0}^{N} u \, \mathrm{d}N + \frac{1}{2}\left(u_0 + \frac{u_0}{N^0}N\right)(N - N^0); \tag{46}$$

where u_0 and N^0 represent the displacement and load at the critical state. A standard integration yields

$$\begin{aligned}\Delta\Phi = &-\frac{N^2 u^{(2)}}{2N^{(2)}} + \frac{\left(N^{(1)2} + 4N \cdot N^{(2)} - 4N^0 N^{(2)}\right)^{\frac{3}{2}}\left(-N^{(2)}u^{(1)} + N^{(1)}u^{(2)}\right)}{12N^{(2)3}} \\ &- \frac{N\left(2N^{(2)2}u^0 - N^{(1)}N^{(2)}u^{(1)} + N^{(1)2}u^{(2)} - 2N^0 N^{(2)}u^{(2)}\right)}{2N^{(2)2}} \\ &+ \frac{12N^0 N^{(2)3}u^0 + N^{(1)3}N^{(2)}u^{(1)} - 6N^0 N^{(1)}N^{(2)2}u^{(1)} - N^{(1)4}u^{(2)} + 6N^0 N^{(1)2}N^{(2)}u^{(2)} - 6N^{02}N^{(2)2}u^{(2)}}{12N^{(2)3}} \\ &+ \frac{1}{2}\left(u_0 + \frac{u_0}{N^0}N\right)(N - N^0).\end{aligned} \tag{47}$$

The energy release rate can thus be calculated with the aid of Eq. (4) by evaluating $\Delta\Phi$ and $\Delta A = B\Delta\ell$ between two infinitesimally close equilibrium states. Using the J-integral calculation, we obtain

$$\begin{aligned}P^* &= \frac{t}{T}\left(N^{(1)} + \frac{6H}{T^2}M_{\mathrm{b}}^{(1)}\right)\varepsilon + \frac{t}{T}\left(N^{(2)} + \frac{6H}{T^2}M_{\mathrm{b}}^{(2)}\right)\varepsilon^2 + \frac{t}{T}\left(N^{(3)} + \frac{6H}{T^2}M_{\mathrm{b}}^{(3)}\right)\varepsilon^3 + \mathrm{O}(\varepsilon^4) \\ &= P^{*(1)}\varepsilon + P^{*(2)}\varepsilon^2 + P^{*(3)}\varepsilon^3 + \mathrm{O}(\varepsilon^4),\end{aligned}$$

$$\begin{aligned}M^{\mathrm{u}} &= \left(-M_{\mathrm{d}}^{(1)} - M_{\mathrm{b}}^{(1)}\frac{t^3}{T^3}\right)\varepsilon + \left(-M_{\mathrm{d}}^{(2)} - M_{\mathrm{b}}^{(2)}\frac{t^3}{T^3}\right)\varepsilon^2 + \left(-M_{\mathrm{d}}^{(3)} - M_{\mathrm{b}}^{(3)}\frac{t^3}{T^3}\right)\varepsilon^3 + \mathrm{O}(\varepsilon^4) \\ &= M^{\mathrm{u}(1)}\varepsilon + M^{\mathrm{u}(2)}\varepsilon^2 + M^{\mathrm{u}(3)}\varepsilon^3 + \mathrm{O}(\varepsilon^4),\end{aligned}$$

$$\begin{aligned}M^{\mathrm{l}} &= \left(-M_{\mathrm{s}}^{(1)} - M_{\mathrm{b}}^{(1)}\frac{t^3}{T^3}\right)\varepsilon + \left(-M_{\mathrm{s}}^{(2)} - M_{\mathrm{b}}^{(2)}\frac{t^3}{T^3}\right)\varepsilon^2 + \left(-M_{\mathrm{s}}^{(3)} - M_{\mathrm{b}}^{(3)}\frac{t^3}{T^3}\right)\varepsilon^3 + \mathrm{O}(\varepsilon^4) \\ &= M^{l(1)}\varepsilon + M^{l(2)}\varepsilon^2 + M^{l(3)}\varepsilon^3 + \mathrm{O}(\varepsilon^4),\end{aligned} \tag{48}$$

therefore, the energy release rate G can be expressed by

$$G = J = \frac{1}{2B}\left[\frac{T(1-\nu^2)}{EBtH}P^{*2} + \frac{M^{u2}}{D_{\mathrm{d}}} + \frac{M^{l2}}{D_{\mathrm{s}}}\right]. \tag{49}$$

On the other hand, in the context of an asymptotic formulation, we obtain the following expression

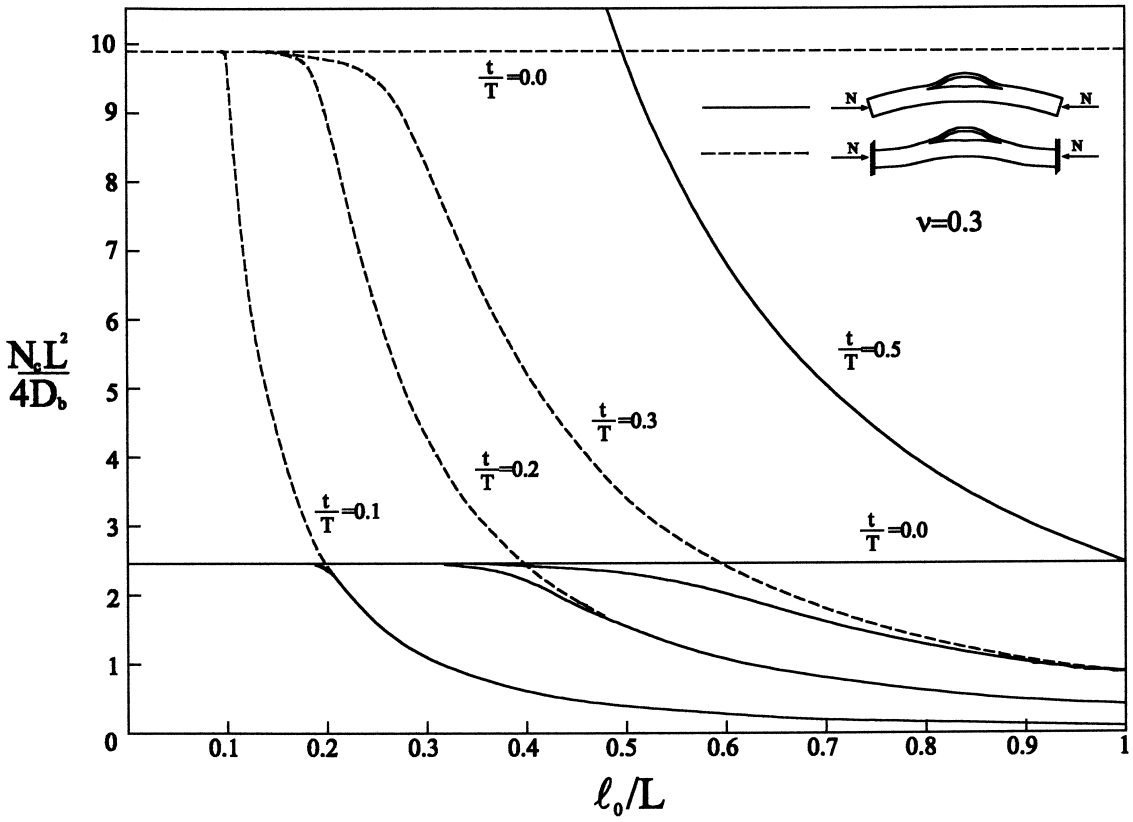

Fig. 10. Buckling load as a function of the delamination length for various t/T ratios.

$$G = J = J^{(2)}\varepsilon^2 + J^{(3)}\varepsilon^3 + J^{(4)}\varepsilon^4 + \mathrm{O}(\varepsilon^5), \tag{50}$$

where

$$J^{(2)} = \frac{1}{2B}\left[\frac{T(1-\nu^2)}{EBtH}P^{*(1)2} + \frac{M^{u(1)2}}{D_\mathrm{d}} + \frac{M^{l(1)2}}{D_\mathrm{s}}\right], \tag{51}$$

$$J^{(3)} = \frac{1}{2B}\left[\frac{T(1-\nu^2)}{EBtH}2P^{*(1)}P^{*(2)} + \frac{2M^{u(1)}M^{u(2)}}{D_\mathrm{d}} + \frac{2M^{l(1)}M^{l(2)}}{D_\mathrm{s}}\right], \tag{52}$$

$$J^{(4)} = \frac{1}{2B}\left[\frac{T(1-\nu^2)}{EBtH}\left(P^{*(2)2} + 2P^{*(1)}P^{*(3)}\right) + \frac{\left(M^{\mathrm{u}(2)2} + 2M^{\mathrm{u}(1)}M^{\mathrm{u}(3)}\right)}{D_\mathrm{d}} + \frac{\left(M^{l(2)2} + 2M^{l(1)}M^{l(3)}\right)}{D_\mathrm{s}}\right]. \tag{53}$$

It follows from our numerical investigation that the results corresponding to Eq. (49) involving second order stress terms are very similar to those obtained employing the fourth order equation (50).

It should be noted that if the asymptotic expansions (48) are performed up to the second order terms, the energy release rate (50) must be coherently taken up to the third order term. In this way, the complete effects of second order stress terms is not considered and third order stress terms are also not incorporated in the energy release rate evaluation which, when a local stress criterion is employed, must be founded on a more accurate asymptotic expansion. This determines imprecise results as shown in Figs. 11 and 12, where the dashed curves represent the results based on the third order approximation of G. In particular, it can be observed that these approximations, give very imprecise results for low values of the t/T parameter. This because third order term $J^{(3)}$ approaches zero as $t/T \to 0$ ($P^{*(1)}$, $M^{u(2)}$, $M^{l(2)} \to 0$) and the effect of second order terms on G are completely neglected.

In the following figures short delaminations have not been considered, because the ultimate axial load capacity is dominated by the initial postbuckling behaviour and not by the delamination growth. The non-dimensional axial load N/N_c (N_c being the critical load) is reported in Figs. 11 and 12, versus the dimensionless transverse central deflection w/L, for two values of the adimensionalized energy release rate $\bar{G}_0 = \ell_0^2 B\Gamma/D_d\pi^4$ (selected to embrace the range of variation in actual laminates, i.e. 140–1400 N/m).

3.2. Thin film–thick column and symmetric split models

Results relative to the simplified schemes of thin film, thick column and symmetric split models are now presented by introducing assumptions on the plate deformation. More precisely, a plate with thickness parameters t and T is considered such that transverse deflections of the upper delaminated layer only occur (Fig. 3).

In this case, the asymptotic expressions of load, displacements and stresses can be obtained by using the results of the elastica for the buckled layer. The parametric form of the force–displacement relation, by enforcing compatibility of axial displacements and equilibrium condition, is

$$N = N_c + N_2\varepsilon^2 + N_4\varepsilon^4 + O(\varepsilon^6), \tag{54}$$

$$u_L = u_0 + u_2\varepsilon^2 + u_4\varepsilon^4 + O(\varepsilon^6), \tag{55}$$

while the bending moment at the delamination end is

$$M^{(1)} = M_1\varepsilon + M_3\varepsilon^3 + O(\varepsilon^5), \tag{56}$$

where

$$u_0 = \frac{NL(1-\nu^2)}{EBT},\ N_c = N_c^{(1)}\frac{T}{t},\ N_c^{(1)} = \frac{\pi^2 EBt^3}{3\ell^2(1-\nu^2)},\ M_1 = \frac{EBt^3\pi}{6(1-\nu^2)\ell},\ M_3 = \frac{EBt^3\pi}{288(1-\nu^2)\ell},$$

$$N_2 = N_2^{(1)}\frac{T}{t} + \frac{EB(T-t)}{\ell(1-\nu^2)}u_2^{(1)},\ N_2^{(1)} = \frac{1}{8}N_c^{(1)},\ u_2^{(1)} = \frac{\ell}{4},\ u_2 = \frac{t}{T}u_2^{(1)},$$

$$N_4 = N_4^{(1)}\frac{T}{t} + \frac{EB(T-t)}{\ell(1-\nu^2)}u_4^{(1)},\ N_4^{(1)} = \frac{17}{1536}N_c^{(1)},\ u_4^{(1)} = -\frac{5\ell}{384},\ u_4 = \frac{t}{T}u_4^{(1)},$$

in which the superscript (1) denotes the upper layer. In addition, the central transverse deflection w of the delaminated layer is:

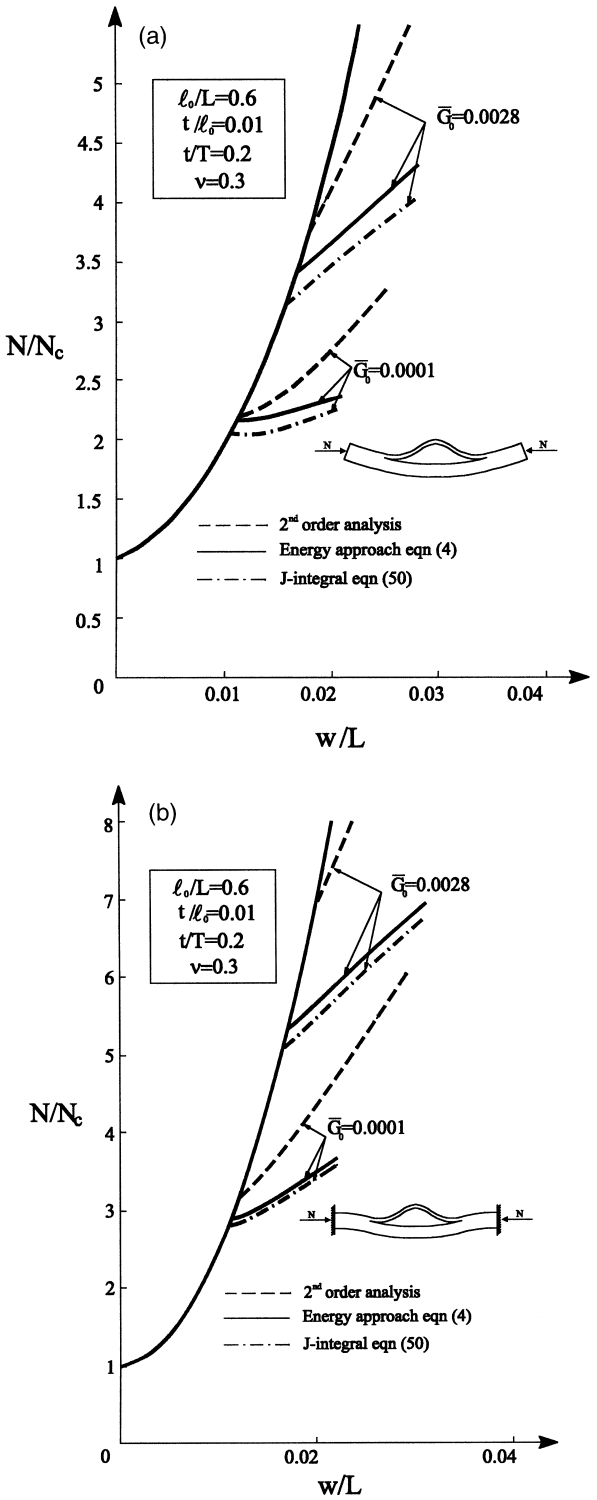

Fig. 11. (a) N–w delamination curves for $s = 3$, (b) N–w delamination curves for $s = 3$.

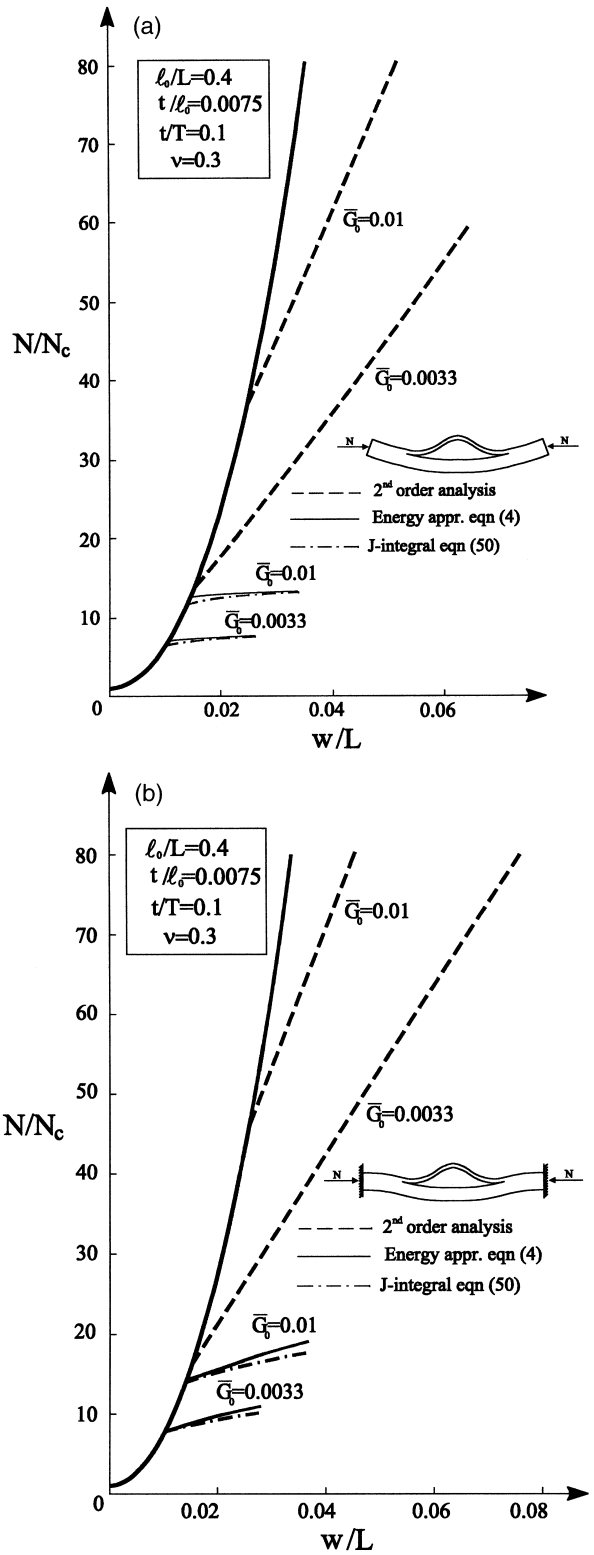

Fig. 12. (a) N–w delamination curves for $s = 4$ (b) N–w delamination curves for $s = 4$.

$$w = \frac{\varepsilon \ell}{\pi} - \frac{5}{48\pi}\varepsilon^3 + \mathrm{O}(\varepsilon^5).$$

In this case the delamination condition (9) can be applied by evaluating the increment of the total potential energy $\Delta\Phi$ with the help of Eq. (6) or, alternatively, by integrating the dashed area of Fig. 4.

If we take the asymptotic expansions (54) and (55) up to $\mathrm{O}(\varepsilon^2)$ terms, the following expression for the energy release rate is found

$$G = \frac{N_c^{(1)}}{4B}\left\{2\varepsilon^2 + \left[\frac{3}{16} + \frac{3}{8\pi^2}\left(\frac{\ell}{t}\right)^2 \frac{T-t}{T}\right]\varepsilon^4\right\}. \tag{57}$$

The same expression of G can also be obtained by considering Eq. (6) up to $\mathrm{O}(\varepsilon^4)$.

However, if terms up to $\mathrm{O}(\varepsilon^4)$ are taken into account, we obtain

$$G = \frac{N_c^{(1)}}{4B}\left\{2\varepsilon^2 + \left[\frac{1}{12} + \frac{3}{8\pi^2}\left(\frac{\ell}{t}\right)^2 \frac{T-t}{T}\right]\varepsilon^4 + \mathrm{O}(\varepsilon^6)\right\}, \tag{58}$$

and the same expression of G is again obtained taking into account terms up to $\mathrm{O}(\varepsilon^6)$ in Eq. (6).

If the J-integral concept is now applied, only the stress resultant terms shown in Fig. 13 are considered, under the condition that the sublaminate exhibits small curvature in comparison with the delaminated layer. These stresses are

$$P^* = \frac{t}{T}N - N^{(1)} = P_2^*\varepsilon^2 + P_4^*\varepsilon^4 + \mathrm{O}(\varepsilon^6) = \frac{t}{T}\frac{EB(T-t)}{\ell(1-\nu^2)}u_2^{(1)}\varepsilon^2 + \frac{t}{T}\frac{EB(T-t)}{\ell(1-\nu^2)}u_4^{(1)}\varepsilon^4 + \mathrm{O}(\varepsilon^6),$$

$$M^{\mathrm{u}} = M^{(1)} = M_1^u\varepsilon + M_3^u\varepsilon^3 + \mathrm{O}(\varepsilon^5) = \frac{EBt^3}{12(1-\nu^2)\ell}\left(2\pi\varepsilon + \frac{\pi}{24}\varepsilon^3 + \mathrm{O}(\varepsilon^5)\right). \tag{59}$$

Let us examine the influence of the various terms in the asymptotic expansion of P^* and M^{u} in detail. If terms up to $\mathrm{O}(\varepsilon^2)$ in Eqs. (59) are taken into account, we obtain

$$G = J = \frac{1-\nu^2}{2BE}\left[\frac{T}{BtH}(P^*)^2 + \frac{12}{Bt^3}(M^u)^2\right] = \frac{N_c^{(1)}}{4B}\left\{2\varepsilon^2 + \left[\frac{3}{8\pi^2}\left(\frac{\ell}{t}\right)^2 \frac{T-t}{T}\right]\varepsilon^4\right\}. \tag{60}$$

This expression is different from the corresponding Eq. (57) because the contribution of the third order stress term M_3 is completely neglected. If this contribution is accounted for (i.e. the asymptotic expansion is fully introduced in Eq. (10)), the following expression for the energy release rate is found

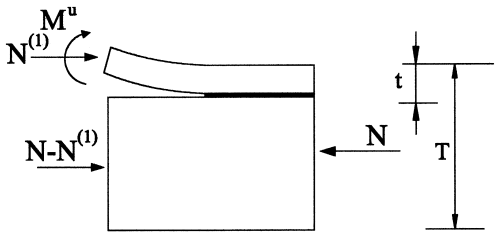

Fig. 13. Stresses at the crack tip.

$$G = J = \frac{N_c^{(1)}}{4B}\left\{2\varepsilon^2 + \left[\frac{1}{12} + \frac{3}{8\pi^2}\left(\frac{\ell}{t}\right)^2 \frac{T-t}{T}\right]\varepsilon^4 + O(\varepsilon^6)\right\}, \tag{61}$$

which coincides with Eq. (58). The agreement between Eqs. (58) and (61) is due to the coherence of the asymptotic expansions employed.

In essence, the result expressed by Eq. (60) has been obtained by Chai et al. (1981). This result, although it does not account for the third order bending term, is sufficiently accurate to model the mechanical behaviour of the narrow-plate example. This is due to the flat postbuckling equilibrium path of the structure.

For this simplified model we give the exact solution which is compared with the asymptotic analysis results. Using the results of elastica, hence the exact dependence through elliptic functions of load and deformation parameters in terms of the distortion parameter ε of the clamped delaminated layer, and applying compatibility and equilibrium requirements we obtain

$$N = N^{(1)}\frac{T}{t} + \frac{EB(T-t)}{(1-\nu^2)}\left(1 - \frac{2E(\pi,k) - F(\pi,k)}{F(\pi,k)}\right), \tag{62}$$

$$u_L = \frac{NL(1-\nu^2)}{EBT} + L\left(1 - \frac{2E(\pi,k) - F(\pi,k)}{F(\pi,k)}\right)\frac{t}{T}, \tag{63}$$

where

$$N^{(1)} = \frac{EBt^3}{12(1-\nu^2)}\frac{4F(\pi,k)}{\ell^2} \text{ and } k = \sin\left(\frac{\varepsilon}{2}\right).$$

Therefore, we can write

$$P^* = \frac{t}{T}N - N^{(1)} = \frac{t}{T}\frac{EB(T-t)}{(1-\nu^2)}\left(1 - \frac{2E(\pi,k) - F(\pi,k)}{F(\pi,k)}\right),$$

$$G = J = \frac{1-\nu^2}{2BE}\left\{\frac{T}{BtH}\left[P^*(k)\right]^2 + \frac{12}{Bt^3}\left[M^u(k,\ell)\right]^2\right\},$$

$$M^u = M^{(1)} = \frac{EBt^3}{3\ell(1-\nu^2)}\sin\left(\frac{\alpha}{2}\right)F(\pi,k). \tag{64}$$

The influence of the thickness/length ratio t/ℓ_0 and the adhesion energy parameter $\bar{G}_0 = B\ell^2\Gamma/D_u\pi^2$, where $D_u = EBt^3/12(1-\nu^2)$, on the delamination growth path is shown in Figs. 14 and 15. The relative shortening u_L/L and the relative deflection w/L are driven until the complete delamination of layers is reached. For the adhesion energy parameter $\bar{G}_0 = B\ell^2\Gamma/D_u\pi^2$, two values have been considered (representative of the interlaminar toughness of the actual laminates: 140–1400 N/m). For a fixed value of the critical energy release rate, utilizing the delamination condition leads to a relation between the distortion parameter ε and the current delamination length, and thus to the delamination growth path.

It can be concluded from Figs. 14 and 15 that the thick column model shows a complex behaviour. In fact, it exhibits a stable behaviour only for relative high values of the thickness–length ratio and of the adhesion energy parameter, while an unstable behaviour can be found for low values of these parameters. Moreover, it can be stated from numerical experiments that the various approximations introduced in the asymptotic analysis (Eqs. (57), (58), and (60)) give negligible differences with respect to

the exact solution. Hence, in Figs. 14 and 15 only numerical results relative to Eq. (57), i.e. the energy approach, (which also represents the best approximation of the problem) are shown.

As far as the limit case of the symmetric split model is concerned, it can be shown that the relevant governing equations can be obtained from those of the thick column model taking $t/T = 1$ in the relative equations.

On the other hand, the limit case of thin film model can be obtained from the thick column model in the limit $t/T \to 0$.

In order to investigate the influence of the various approximations introduced in the analyses of the symmetric split model, plots of the delamination growth path are shown in Fig. 16. Even in this case two values of the adhesion energy parameter $\bar{G}_0 = B\ell^2\Gamma/D_u\pi^2$ have been chosen to represent the interlaminar toughness of the current laminates.

Fig. 16 shows that the introduced approximations lead to a practically coincident path, in fact the load at the onset of delamination is very near to the critical value. The difference is just appreciable when a decrease in the thickness-length ratio increases the delamination growth load. In this case only the delamination condition is influenced by a more advanced postbuckling phase. Furthermore, the best approximation to the exact solution in terms of delamination growth path seems to be the total potential increment variation with a second order analysis (Bruno, 1988).

We can conclude that for the symmetric split and thick column problems the refinements introduced in the analytical developments do not practically improve the solution. This is related to the flat

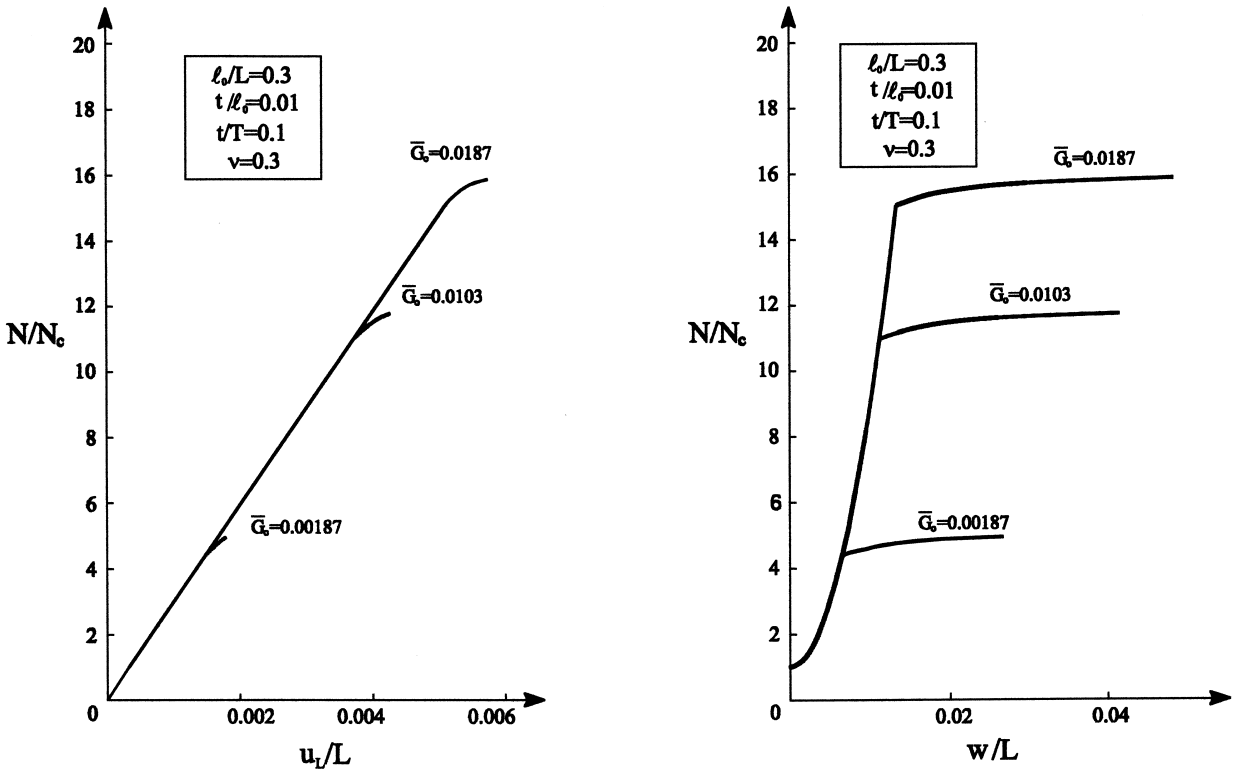

Fig. 14. Thick column model: influence of $\bar{G}_0$ for $t/T = 0.1$.

postbuckling behaviour of the buckled layer. On the contrary, we will see for other examples characterized by a very stiff postbuckling (for instance the two-dimensional circular plate) that the solution is strongly affected by the above-discussed approximations.

3.2.1. Convergence of the general model to the thin film model

Numerical results show the convergence of the general model to the simplified thick-column model, when $t/T \to 0$. A delaminated plate with a fixed value $\ell_0/L = 0.5$ of the initial defect ratio is considered and it is also assumed that the slenderness parameter s goes from 2.5 to 10.

The behaviour of the plate model is examined by evaluating the differences $e_G = (G_{gen} - G_{thick})/G_{gen}$, between the energy release rate G_{gen} of the general model and G_{thick} of the thick-column model. These results are shown in Fig. 17, where the relative quantity e_G is plotted versus the thickness parameter t/T.

It can be observed that the general model and the thick column model tend to coincide for a decreasing ratio t/T, and that the general model is less stiff than the other. Moreover, in the case of clamped plate, the agreement is more satisfactory than in the simply supported case for lower t/T ratios. As a matter of fact, the same behaviour of long delaminations in the case of clamped boundary condition is found for lower slenderness with respect to the simply supported case.

Moreover, it becomes evident from Fig. 17 that the general model predicts a much higher energy release rate than the thick column model. In the case of simply supported plate the thick column approximation can be applied only in an initial stage of postbuckling.

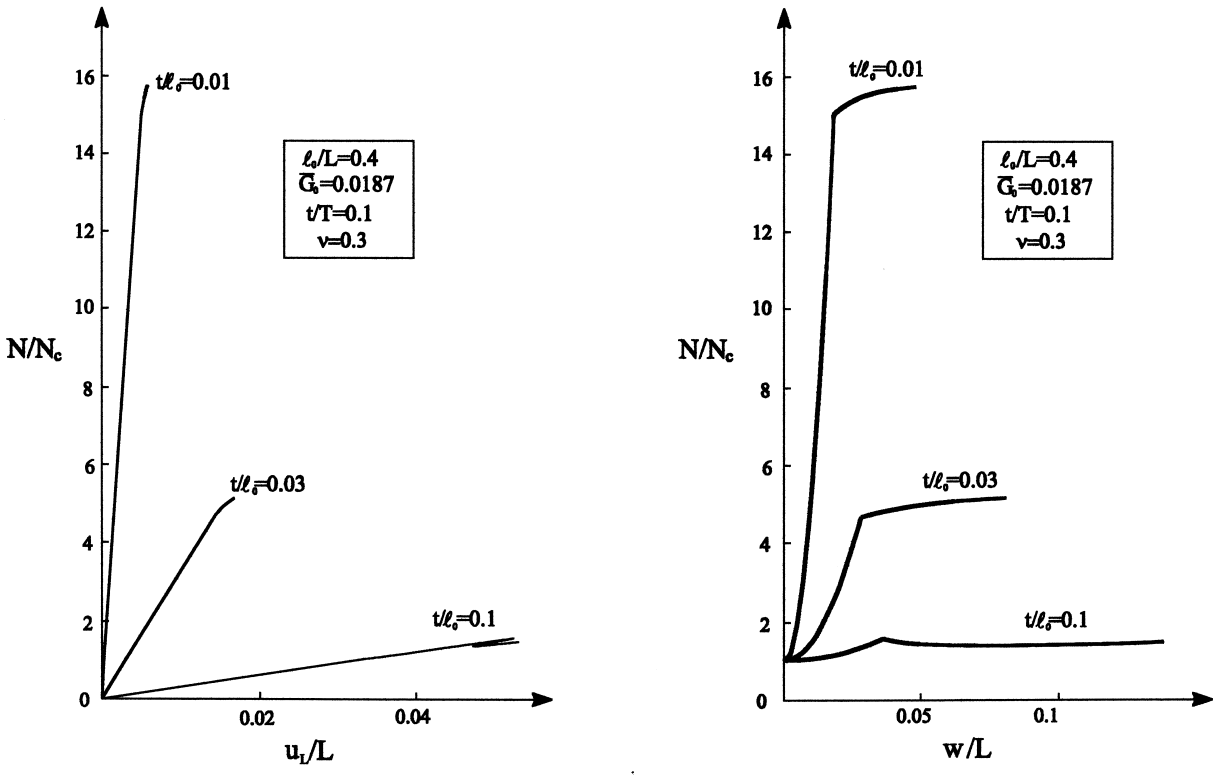

Fig. 15. Thick column model: influence of t/ℓ_0 for $t/T = 0.1$.

Delamination growth curves are compared in Fig. 18, and it is clear that when the relative slenderness parameters become larger, the general model tends towards the simplified one.

As far as the general plate model is concerned, we can conclude that the delaminated plate can exhibit essentially two behaviours:

- for thick and short delaminations ($s < 2\bar{\ell}^*$), buckling is global at a load close to the critical load of the perfect plate with possibility of crack closure,
- for long and thin delaminations ($s > 2\bar{\ell}^*$), buckling is local (i.e. only the delaminated layer buckles) and the critical load of the whole plate is drastically reduced.

While in the former case the plates follows an unstable elastic postbuckling behaviour, in the latter the maximum axial load carrying capacity is dominated by the delamination growth.

Moreover, it appears from our results that the simplified models can be appropriately used to model the behaviour of plates containing long delaminations. On the contrary, for short delaminations the simplified models based on a local buckling hypothesis do not capture the actual behaviour of the plate. This is because a global buckling occurs and thus a strong influence of the boundary conditions is found.

When a Griffith criterion is adopted, the delamination growth is generally catastrophic, except for long delaminations. Moreover, the clamped boundary condition shows greater stability in the delamination growth.

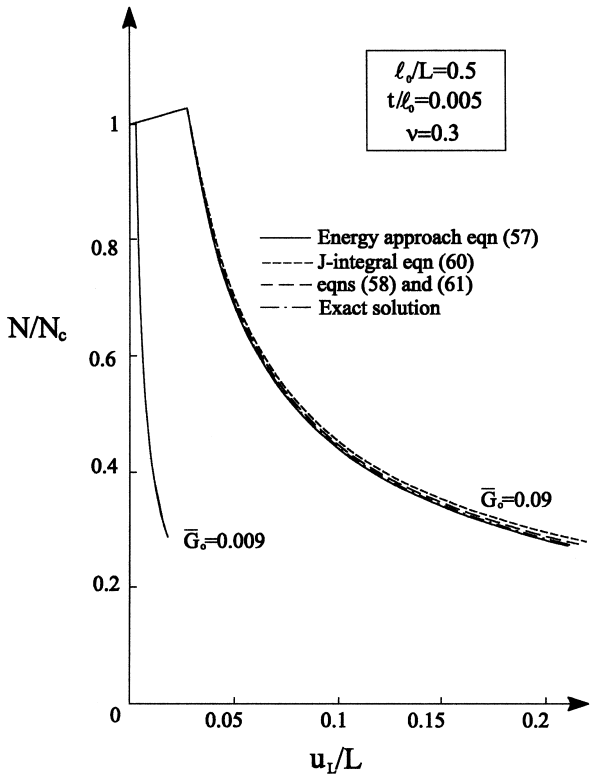

Fig. 16. Symmetric split model: influence of $\bar{G}_0$ on delamination growth paths.

4. Circular plate model

A circular two-layers plate with radius $\bar{R}$ debonded over a penny-shaped region of radius R is now considered (Fig. 19). For this structural model, a closed form solution may be hard to obtain, at least in the general case in which a global buckling of the plate occurs. Therefore, we analyze here only the symmetric split, thick column and thin film simplified models.

The postbuckling behaviour of the circular plate is modelled employing the von Kàrmàn plate theory in the form given by Thompson and Hunt (1973).

It will be shown that for this structure the accuracy in the evaluation of the asymptotic terms involved in the energy release rate calculation and in the postbuckling stress and deformation parameters, are of great importance.

The governing equations of the thick column model are determined in a way similar to that employed in the previous section. Finally, the symmetric split and thin film model approximations are obtained from the thick column model by setting $t/T = 1$ and $t/T \to 0$, respectively.

From Thompson and Hunt (1973) the axial stress $N_{\mathrm{R}}^{(1)}$ and the inward axial displacement u_{R} for the

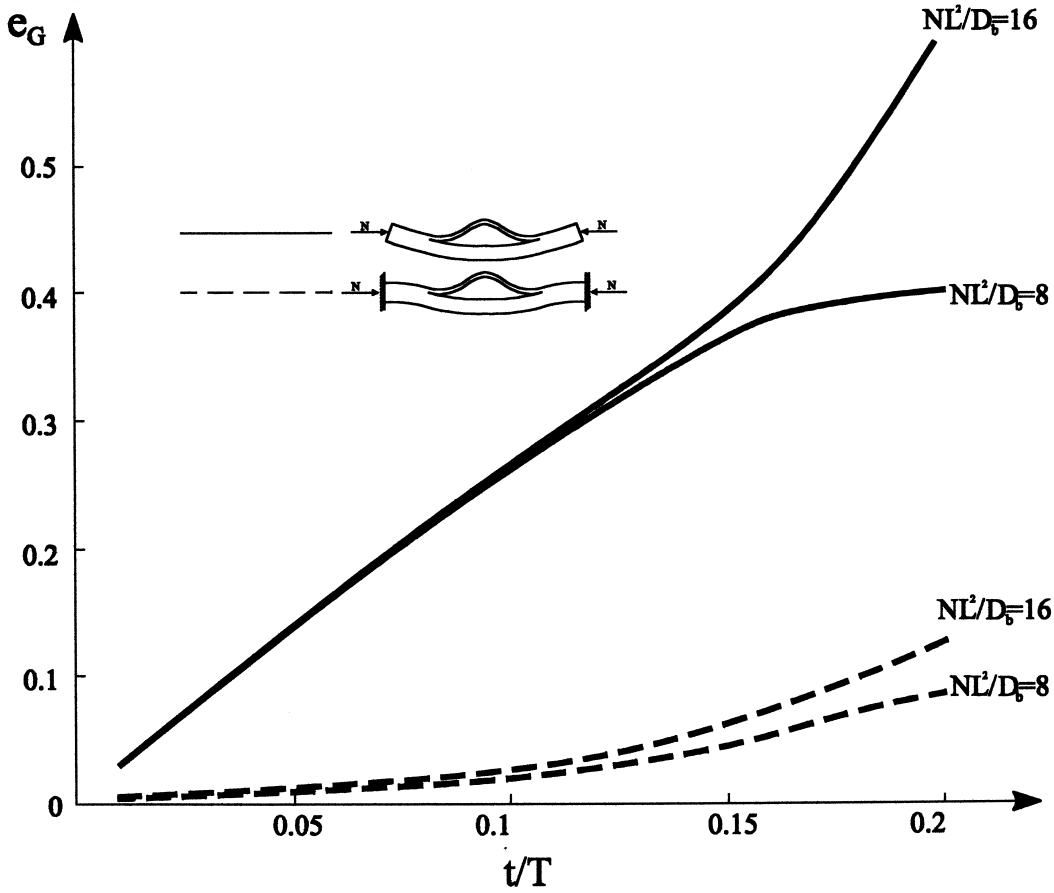

Fig. 17. Relative difference $e_{\mathrm{G}} = (G_{\mathrm{gen}} - G_{\mathrm{thick}})/G_{\mathrm{gen}}$, for the energy release rate. Different values of the parameter NL^2/D_{b} are considered.

upper buckled layer at the boundary of radius R can be written as

$$N_{\mathrm{R}}^{(1)} = N_{\mathrm{RC}}^{(1)} + N_{\mathrm{R2}}^{(1)}\xi^2, \tag{65}$$

$$u_{\mathrm{R}} = \frac{N_{\mathrm{R}}^{(1)}(1-\upsilon)}{Et}R + u_{2\mathrm{R}}^{(1)}\xi^2, \tag{66}$$

where,

$$N_{\mathrm{RC}}^{(1)} = 14.68\frac{D}{R^2}, \qquad N_{\mathrm{R2}}^{(1)} = 0.2049N_{\mathrm{RC}}^{(1)}, \tag{67}$$

$$u_{2\mathrm{R}}^{(1)} = \frac{\gamma^2 R J_0^2(\gamma R)}{4\left[J_0(\gamma R)-1\right]^2}t^2, \qquad \gamma = \sqrt{\frac{N_{\mathrm{RC}}^{(1)}}{D}} = \frac{3.832}{R}. \tag{68}$$

In Eqs.(65)–(68) we denote by $D = Et^3/12(1-\nu^2)$ the bending stiffness of the delaminated layer, t being the thickness, E and ν the modulus of elasticity and the Poisson's ratio, respectively, and J_0 the zeroth-order Bessel function of the first kind. The dimensionless displacement parameter ξ is

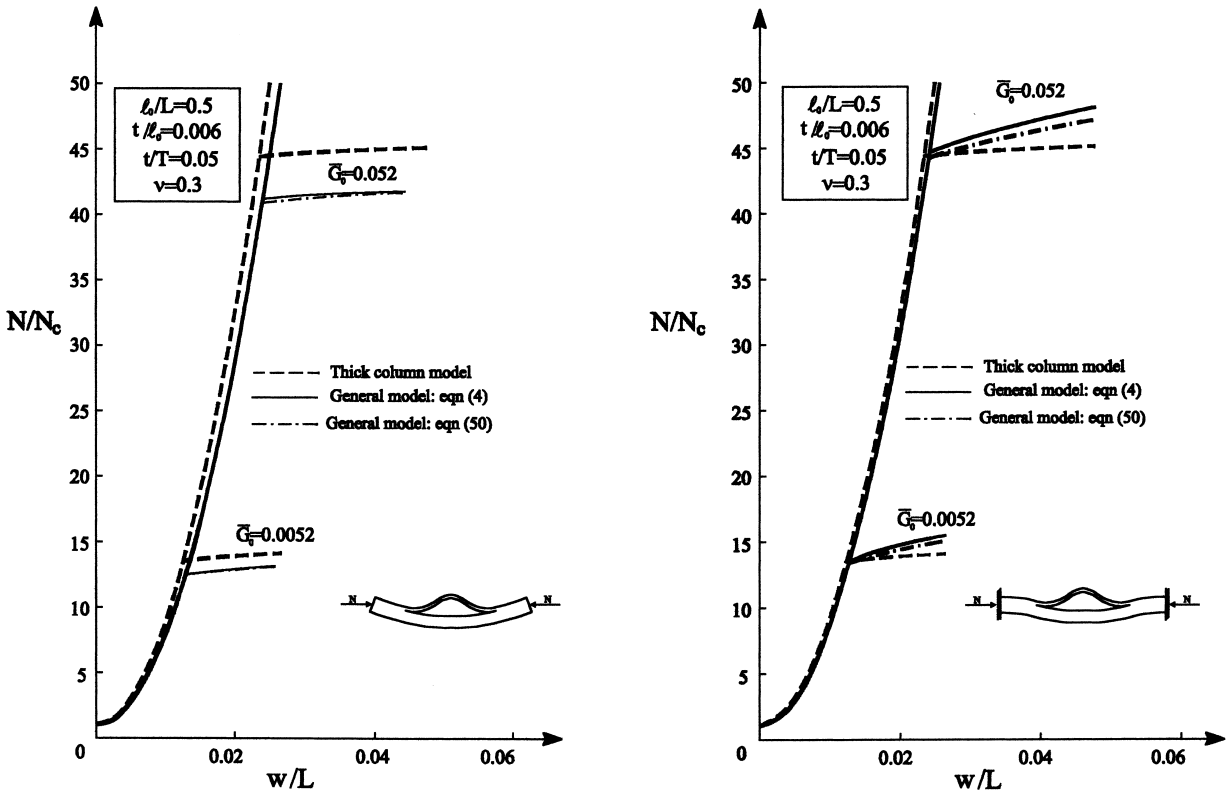

Fig. 18. Comparison in the N–w delamination growth paths for $s = 10$ and different models: (a) simply supported plate and (b) clamped plate.

$$\xi = \frac{w}{t},$$

where w is the central transverse deflection of the upper layer.

The axial force $N_R^{(2)}$ acting on the lower layer is written as

$$N_R^{(2)} = \frac{E(T-t)}{R(1-\upsilon)} u_R. \tag{69}$$

The total axial force $N_R = N_R^{(1)} + N_R^{(2)}$ at the boundary of radius R, utilizing Eqs. (65) and (66) becomes

$$N_R = N_{RC} + N_{R2}\xi^2, \tag{70}$$

where

$$N_{RC} = N_{RC}^{(1)} \frac{T}{t}, \qquad N_{R2} = \left[0.2049 N_{RC} + u_{2R}^{(1)} \frac{E(T-t)}{R(1-\upsilon)} \right], \tag{71}$$

while the axial displacement at the boundary of radius R, is

$$u_R = \frac{N_R(1-\upsilon)}{ET} R + \frac{t}{T} u_{2R}^{(1)} \xi^2. \tag{72}$$

Now, the annular plate with inner radius R and outer radius $\bar{R}$ is analyzed. The axial displacement can be related to the external compression N through the following expression

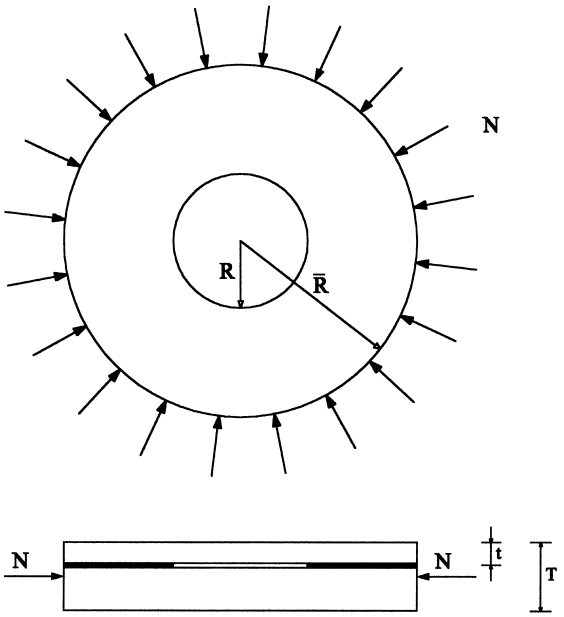

Fig. 19. Circular plate scheme.

$$u(r)=\frac{1}{ET}\left[\frac{1+\upsilon}{r}\frac{R^2(N-N_{\mathrm{R}})}{1-\dfrac{R^2}{\bar{R}^2}}-\frac{N_{\mathrm{R}}\dfrac{R^2}{\bar{R}^2}-N}{1-\dfrac{R^2}{\bar{R}^2}}(1-\upsilon)r\right],\quad\text{with}\quad R\le r\le\bar{R}. \tag{73}$$

From Eqs. (70)–(73) we obtain

$$N=N_{\mathrm{c}}+N_2\xi^2, \tag{74}$$

where

$$N_{\mathrm{c}}=N_{\mathrm{RC}}, \tag{75}$$

$$N_2=N_{\mathrm{RC}}\left[0.2049+\frac{3J_0^2(\gamma R)}{\left[J_0(\gamma R)-1\right]^2}\left(1-\frac{t}{T}\right)(1+\upsilon)+0.4087(1-\upsilon^2)\right.$$
$$\left.\times\left(1-\frac{R^2}{\bar{R}^2}\right)\frac{t}{T}\frac{J_0^2(\gamma R)}{4\left[J_0(\gamma R)-1\right]^2}(\gamma R)^2\right], \tag{76}$$

and for the in-plane outer boundary displacement $u_{\bar{\mathrm{R}}}$

$$u_{\bar{\mathrm{R}}}=\frac{N(1-\upsilon)}{ET}\bar{R}+\frac{t^2}{\bar{R}^2}\frac{J_0^2(\gamma R)}{4\left[J_0(\gamma R)-1\right]^2}(\gamma R)^2\frac{t}{T}\xi^2. \tag{77}$$

Griffith's criterion for the uniform expansion of the delamination takes the form

$$2\pi R\Gamma=-\frac{\partial\Delta\Phi}{\partial R}, \tag{78}$$

where the fourth order approximation of the total potential energy in terms of the applied load via a second order analysis (i.e. Eqs. (74) and (77) or Eq. (6) up to the fourth order terms) is

$$\Delta\Phi=-\frac{1}{2}2\pi\bar{R}\frac{(N-N_{\mathrm{c}})^2}{N_2}\bar{R}\left(\frac{t}{\bar{R}}\right)^2\frac{J_0^2(\gamma R)}{4\left[J_0(\gamma R)-1\right]^2}(\gamma R)^2\frac{t}{T}. \tag{79}$$

Using Eq. (78) and the numerical value of the Bessel function $J_0(\gamma R)$, the delamination condition is expressed in the form

$$1.21\xi^2+0.605\left[0.2049+0.1236(1-\upsilon^2)\frac{t}{T}+0.2473(1+\upsilon)\left(1-\frac{t}{T}\right)\right]\xi^4=2\beta_0\left(\frac{R}{\bar{R}}\right)^4, \tag{80}$$

where

$$\beta_0=\frac{\Gamma\bar{R}^2}{\bar{\sigma}_{\mathrm{c}}t^3},\qquad\bar{\sigma}_{\mathrm{c}}=14.68\frac{D}{\bar{R}^2t}.$$

Under the assumption of the thin film model ($t/T\to 0$), the external compression and the axial edge displacements become

$$N = N_{RC} + N_2\xi^2,\ u_{\bar{R}} = \frac{N(1-\upsilon)}{ET}\bar{R} \tag{81}$$

where

$$N_2 = N_{RC}\left[0.2049 + \frac{3J_0^2(\gamma R)}{\left[J_0(\gamma R) - 1\right]^2}(1+\upsilon)\right]. \tag{82}$$

Finally, the delamination condition can be written as

$$1.21\xi^2 + 0.605\left[0.2049 + 0.2473(1+\upsilon)\right]\xi^4 = 2\beta_0\left(\frac{R}{\bar{R}}\right)^4. \tag{83}$$

The delamination growth is analyzed by applying the path independent integral concept. In particular, the M-integral is employed in the form of Eq. (8) over a revolution surface bounded by the hatched curve in Fig. 20 (see Yin, 1985) and superposing on the postbuckling solution the following biaxial stress field

$$\sigma_x = \sigma_y = -\frac{N_R}{T}, \tag{84}$$

in the region surrounding the edge of delamination that, due to its continuity, does not affect the stress intensity factors. The energy release rate is thus produced only by the bending moment M^* acting at the tip of the delaminated layer and the axial force P^* defined by

$$P^* = N_R^{(1)} - N_R\frac{t}{T}, \qquad M^* = M_R^{(1)}, \tag{85}$$

and sketched in Fig. 20.

The energy release rate with the application of the M-integral is

$$G = \frac{(1-\upsilon^2)}{2E}\left[\frac{TP^{*2}}{t(T-t)} + 12\frac{M^{*2}}{t^3}\right], \tag{86}$$

which, in the limit $t/T \to 0$, can be written as

$$G = \frac{(1-\upsilon^2)}{2E}\left[\frac{P^{*2}}{t} + 12\frac{M^{*2}}{t^3}\right]. \tag{87}$$

The bending moment at the edge of the delamination can be expressed in the following asymptotic form

$$M^* = M_1^*\xi + M_3^*\xi^3 + \mathrm{O}\left(\xi^3\right). \tag{88}$$

The first order term M_1^* is often assumed to be the main contribution in the delamination condition. But, as it is shown in the following, the third order term M_3^*, although negligible in the case of narrow-plate scheme, dominates the delamination growth behaviour in plate models exhibiting high stiff postbuckling, as for the present case.

The first order term M_1^* is given by (Thompson and Hunt, 1973)

$$M_1^* = D\left(\ddot{w}_1 + \frac{\upsilon}{r}\dot{w}_1\right)t = \frac{\gamma^2 DJ_0(\gamma R)t}{J_0(\gamma R) - 1}; \tag{89}$$

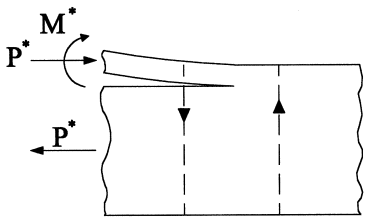

Fig. 20. Equivalent loading system for the calculation of the energy release rate.

while, to obtain the third order term M_3^*, consideration of the third order equation for the transverse deflection is needed. This is a Bessel type equation which, while expanded, gives

$$w_3''' + \frac{w_3''}{r} - \frac{w_3'}{r^2} + \frac{12(1-\upsilon^2)P^c}{Et^3}w_3' = \frac{12}{t^2}\left(v_2' + \frac{w'^2_1}{2} + \upsilon\frac{v_2}{r}\right)w_1' - \frac{12(1-\upsilon^2)P^{(2)}}{2Et^3}w_1', \tag{90}$$

with the following boundary conditions

$$w_3(0) = 0,\ w_3'(0) = 0, \tag{91}$$

$$w_3(R) = 0,\ w_3'(R) = 0, \tag{92}$$

where a prime denotes differentiation with respect to the abscissa r, and the second order load coefficient is $P^{(2)} = 6.017D/R^2t^2$. The linear differential equilibrium Eq. (90) does not admit a closed-form solution and therefore must be numerically solved.

The numerical procedure to be employed has to be suitably chosen to avoid the effects of singularities arising from the second particular solution of the Bessel type equation. To this purpose, an efficient numerical procedure is represented by a collocation type method, which automatically overcomes the singularity effects when a polynomial-like basis is assumed.

Thus, the solution can be approximated by finding a linear combination of linearly independent polynomial functions r^j in the form

$$w_3(r) = \sum_{j=0}^{N} c_j r^j. \tag{93}$$

Finally, we can give the following numerical approximation of the term M_3^*

$$M_3^* = D\left(\ddot{w}_3 + \frac{\upsilon}{r}\dot{w}_3\right)t^3 = Dt^3\sum_{j=2}^{N} j(j-1)c_j r^{j-2}. \tag{94}$$

A comparison between the bending moment calculated including in Eq. (88) the terms up to the first and third order and the exact solution given by Yin (1985) is presented in Figs. 21 and 22. Comparisons are presented for the dimensionless bending moment MR^2/Dt versus the dimensionless axial applied load N/N_c (Fig. 21) and the axial shortening u/u_c (Fig. 22). The strong importance of the third order term M_3^* emerges from the results.

Now we discuss the influence of the terms in the asymptotic expansion of P^* and M^*. In fact, these quantities can be arranged in the following form:

$$\begin{cases} P^* = -\dfrac{Etu_{2R}^{(1)}}{R(1-\upsilon)}\xi^2 = P_2^*\xi^2 + \mathrm{O}(\xi^4) \\ M^* = M_1^*\xi + M_3^*\xi^3 + \mathrm{O}(\xi^5) \end{cases}. \tag{95}$$

If terms up to $\mathrm{O}(\xi^2)$ are considered, i.e. the term M_3^* is neglected, the energy release rate becomes

$$G = \frac{(1-\upsilon^2)}{2E}\left[\frac{P_2^{*2}}{t}\xi^4 + 12\frac{M_1^{*2}}{t^3}\xi^2\right]. \tag{96}$$

On the other hand, it is evident that if Eq. (96) is considered as an asymptotic expansion of G,the fourth order term is incomplete because it does not contain the contribution of the product $M_1^* M_3^* = \mathrm{O}(\xi^4)$. Thus, to obtain a correct fourth order expression for G we have to deal with a third order perturbation analysis, i.e. including M_3^*. This leads to

$$G = \frac{(1-\upsilon^2)}{2E}\left[12\frac{M^{*(1)2}}{t^3}\xi^2 + \left(\frac{P^{*(2)2}}{t} + 24\frac{M^{*(1)}M^{*(3)}}{t^3}\right)\xi^4 + \mathrm{O}(\xi^4)\right]. \tag{97}$$

Comparisons between the delamination growth paths obtained through Eqs. (83), (96), (97) and the exact numerical solution (Yin, 1985) are presented in Figs. 23 and 24. It can be noted that, unlike the narrow plate model, the circular plate behaviour is always found to be unstable for all values of the t/T ratio if Eq. (97) is employed. The same behaviour is found through the exact solution and the energy approach (Eq. (83)). On the contrary, if the incomplete fourth order equation (96) is used, an erroneous stable behaviour of the plate is obtained during the delamination growth for increasing values of the adhesion energy parameter. Thus, the behaviour of the circular plate is found to be sensitive to the bending terms neglected in the fourth order asymptotic coefficient and it becomes therefore necessary to deal at least with a third order analysis.

This can be attributed to the remarkable stiffness of the circular plate during postbuckling.

Considerations similar to those developed for the thin film model can also be reported for the symmetric split model. More precisely, if the M_3^* term is neglected, the following expression of the

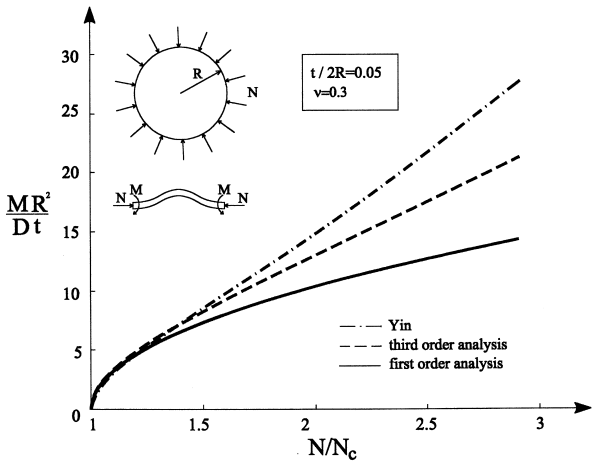

Fig. 21. Bending moment in the postbuckling of a circular plate. Convergence of the perturbation method in terms of the applied load N/N_c.

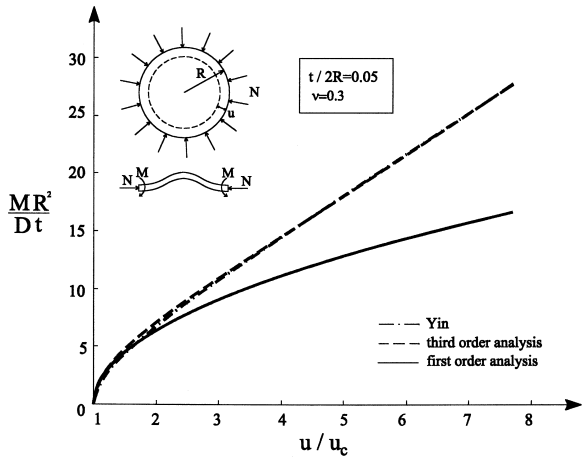

Fig. 22. Bending moment in the postbuckling of a circular plate. Convergence of the perturbation method in terms of the axial shortening u/u_c.

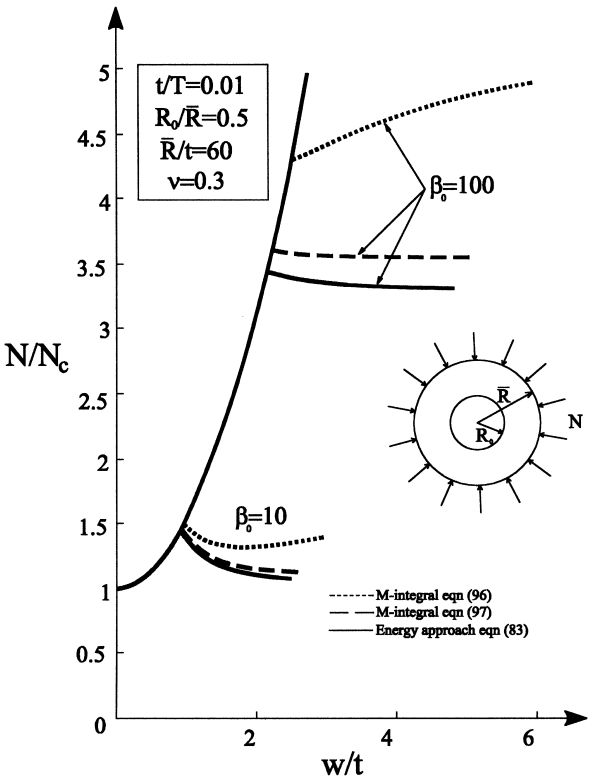

Fig. 23. Delamination behaviour of a circular thin film model. Applied compression N/N_c versus central deflection w/t for constant values of $\beta_0(t/T = 0.01)$.

energy release rate is found

$$G = \frac{M^{*2}}{D} = \frac{1}{D}\left[M_1^{*2}\xi^2 + \mathrm{O}(\xi^4)\right], \tag{98}$$

which is the same reported in Bottega and Maewal (1983). On the other hand, a refined expression of G can be found by accounting for the contribution of the M_3^* term

$$G = \frac{1}{D}\left[M_1^{*2}\xi^2 + 2M_1^*M_3^*\xi^4 + \mathrm{O}(\xi^6)\right]. \tag{99}$$

The behaviour of the models corresponding to Eqs. (80) (with $t/T = 1$), (98) and (99) is shown in Fig. 25, where a comparison with the exact numerical solution of Yin (1985) is proposed for the delamination growth paths. In particular, the dimensionless applied load N/N_c is plotted against the dimensionless axial shortening $u_{\bar{R}}/\bar{R}$. Moreover, the delamination growth paths in terms of the dimensionless applied load N/N_c versus the dimensionless central transverse deflection of the plate w/t is shown in Fig. 26. It can be appreciated that neglecting the fourth order terms in Eq. (99), i.e. considering Eq. (98), leads to an underestimation of the energy release rate. This reflects in predicting a stable delamination growth for sufficiently large values of the adhesion energy parameter β_0, a circumstance in contrast with our results and those obtained by Yin (1985), where a catastrophic delamination growth is always found. Moreover, it can be noted from Fig. 25 that the energy approach solution, Eq. (80), is the best approximation to the exact solution.

It can be finally observed that the M-integral approach in the form of asymptotic expansion, represented by Eq. (99), can only capture the main behavioural features of the delaminated plate. But,

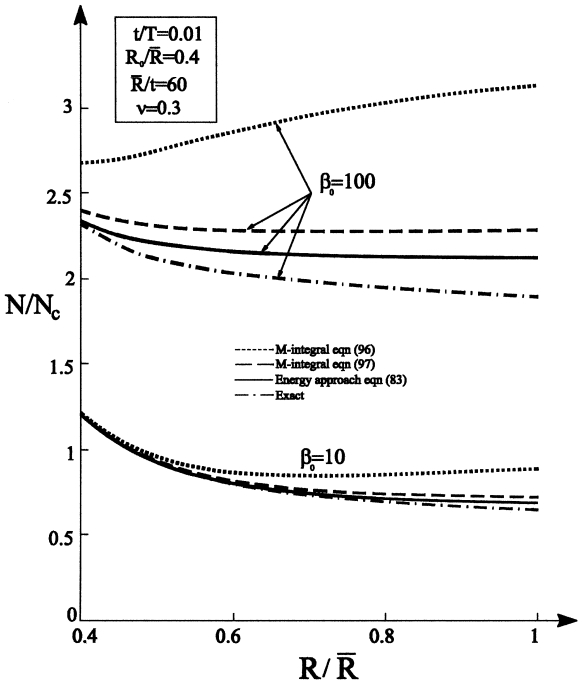

Fig. 24. Thin film model: N/N_c vs. $R/\bar{R}$ for constant values of $\beta_0(t/T = 0.01)$.

this is obtained only if higher order terms, with respect to the energy approach, are included in the asymptotic expansion of variables. Obviously, this determines an increasing effort in calculations.

5. Conclusions

When a Griffith type fracture criterion is employed, essentially two classic methods of analyzing delamination growth behaviour in layered plates are available in fracture mechanics. One is a global approach, the energy method, directly derived from Griffith's theory, and based on energy balance during crack growth. This leads to the definition of the energy release rate concept. The other is a local approach, based on stress intensity factor, which expresses the entity of stress field in the neighbourhood of the crack tip. It is well-known that both methods are substantially equivalent.

In addition to these two approaches, a number of path independent integrals have been proposed to calculate the energy release rate. In applying these integrals along special paths it is found that the energy release rate is a function of the stress resultants acting upon the cross sections adjoining the crack border. Similar results in the form of jump conditions have been found by means of variational statements (see, for instance, Storåkers and Andersson, 1988).

Analytical solutions can be obtained by the global approach and path independent integrals for

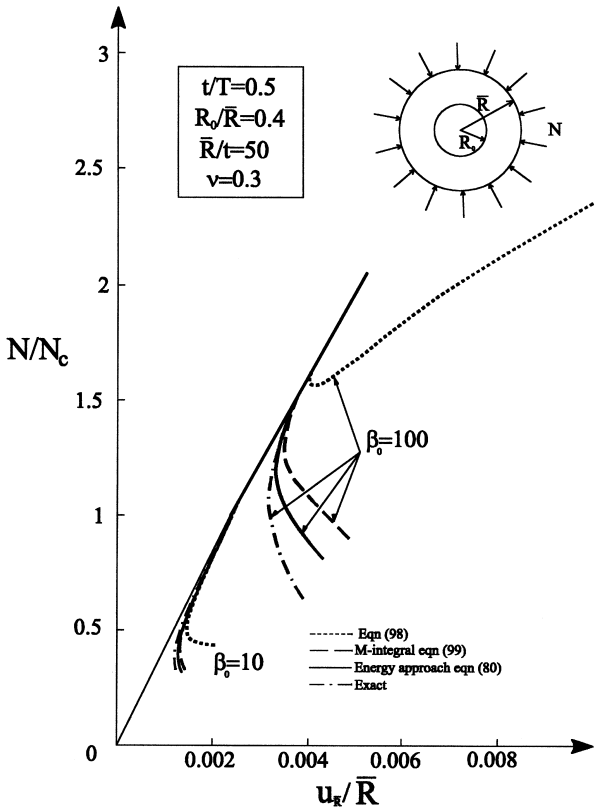

Fig. 25. Delamination behaviour of a two-layer symmetric circular plate. Applied compression N/N_c versus axial shortening $u_{\bar{R}}/\bar{R}$ for constant values of β_0.

appropriate models of damaged laminated plates which allow us investigation of the actual behaviour of delamination growth.

All the aforementioned methods should lead to the same results, but these results turn out to be noticeably influenced by the accuracy of the analysis employed. As a matter of fact, in the case of delamination buckling, a postbuckling solution has to be determined, and its accuracy must be consistent with the stage of the postbuckling path involved in the delamination condition.

In general, with the exception of some simple problems, it is not possible to obtain closed form solutions. Thus, it is necessary to use approximate methods, such as asymptotic techniques.

In this work, an asymptotic method has been used to model the delamination buckling and growth of layered plates by using both the energy and the path-integral approaches. In the latter case the stress resultants at the crack tip are involved in the energy release rate calculation and therefore accurate analyses of higher order are required to obtain a satisfactory evaluation of these stresses. In fact, an inappropriate evaluation of these stresses can lead to very imprecise results, particularly regarding the postbuckling delamination growth.

A perturbative approach has been used to model the delamination buckling, based on an appropriate asymptotic expansion of variables involved in the analysis. A general model of the plate has been analyzed in which an arbitrary buckled configuration involving global and local instabilities can occur. The relevant governing equations of the model are constructed in general asymptotic form and some

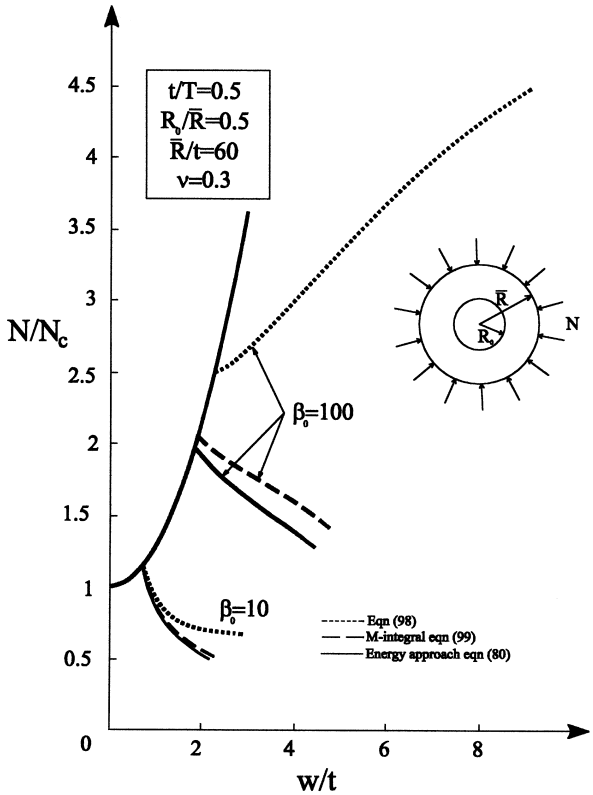

Fig. 26. Delamination behaviour of a two-layer symmetric circular plate. Applied compression N/N_c versus central deflection w/t for constant values of β_0.

numerical results are also given to show the characteristics of the plate behaviour. Based on the same approach, autonomous simplified models of the plate (thick column, thin film and symmetric split models), are also developed.

Comparisons with the various approaches employed to analyze delamination growth behaviour have been presented, both for the narrow plate and for the circular plate model. It can be concluded from our results that when a perturbation analysis is performed, the best way to capture the actual behaviour of a delaminated plate is the global approach with the variation in the advancing delaminated area of the increment of total potential energy. This is true especially when the postbuckling analysis requires a greater accuracy, as in the case of a circular plate, because of its remarkably stiff behaviour.

Acknowledgements

This work was partially supported by Regione Calabria (POP 94/99).

References

Bottega, W.G., Maewal, A., 1983. Delamination buckling and growth in laminates. J. Appl. Mech 50, 184–189.

Britvec, S.-J., 1973. The Stability of Elastic Systems. Pergamon Press, New York.

Bruno, D., 1988. Delamination buckling in composite laminates with interlaminar defects. Theoretical and Applied Fracture Mechanics 9 (2), 145–159.

Bruno, D., Grimaldi, A., 1990. Delamination failure of layered composite plates loaded in compression. Int. J. Solids Structures 26 (3), 313–330.

Budiansky, B., 1974. Theory of buckling and postbuckling behavior of elastic structures. In: Chia Shum, Yih (Ed.), Advances in Applied Mechanics, Vol. 14. Academic Press, New York, pp. 1–65.

Budiansky, B., Rice, J.R., 1973. Conservation laws and energy release rates. J. Appl. Mech 40, 201–203.

Chai, H., Babcock, C.D., Knauss, W.G., 1981. One dimensional modeling of failure in laminated plates by delamination buckling. Int. J. Solids Structures 17 (11), 1069–1083.

Comiez, J.M., Waas, A.M., Shahwan, K.W., 1995. Delamination buckling: experiment and analysis. Int. J. Solids Structures 32 (6/7), 767–782.

Evans, A.G., Hutchinson, J.W., 1984. On the mechanics of delamination and spalling in compressed films. Int. J. Solids Structures 20 (5), 455–466.

Kardomateas, G.A., 1990. Postbuckling characteristics in delaminated Kevlar/Epoxy laminates: an experimental study. J. Composites Technology and Research 12, 85–90.

Kardomateas, G.A., 1993. The initial postbuckling and growth behaviour of internal delaminations in composite plates. J. Appl. Mech 60, 903–910.

Larsson, P.-L., 1991. On delamination buckling and growth in circular and annular orthotropic plates. Int. J. Solids Structures 27 (1), 15–28.

Rice, J.R., 1968. A path independent integral and the approximate analysis of strain concentration by notches and cracks. J. Appl. Mech 90, 379–386.

Sheinman, I., Kardomateas, G.A., 1997. Energy release rate and stress intensity factors for delaminated composite laminates. Int. J. Solids Structures 34 (4), 451–459.

Sheinman, I., Kardomateas, G.A., Pelegri, A.A., 1998. Delamination growth during pre- and postbuckling phases of delaminated composite laminates. Int. J. Solids Structures 35 (1-2), 19–31.

Storåkers, B., Andersson, B., 1988. Nonlinear plate theory applied to delamination in composites. J. Mech. Phys. Solids 36 (6), 689–718.

Thompson, J.M.T., Hunt, G.W., 1973. A General Theory of Elastic Stability. Wiley, New York.

Yin, W.L., 1985. Axisymmetric buckling and growth of a circular delamination in a compressed laminate. Int. J. Solids Structures 21 (5), 503–514.

Yin, W.L., Sallam, S.N., Simitses, G.J., 1986. Ultimate axial load capacity of a delaminated beam-plate. AIAA Jl 24 (1), 123–128.

Yin, W.-L., Wang, J.T.S., 1984. The energy-release rate in the growth of a one-dimensional delamination. J. Appl. Mech 51, 939–941.